



## Attribution of climate change and human activities to streamflow variations with a posterior distribution of hydrological simulations

Xiongpeng Tang<sup>1,2,3</sup>, Guobin Fu<sup>4</sup>, Silong Zhang<sup>1</sup>, Chao Gao<sup>1</sup>, Guoqing Wang<sup>2,3</sup>, Zhenxin Bao<sup>2,3</sup>, Yanli Liu<sup>2,3</sup>, Cuishan Liu<sup>2,3</sup>, Junliang Jin<sup>2,3</sup>

5 <sup>1</sup>Beijing Normal University at Zhuhai, Zhuhai 519087, China

<sup>2</sup>State Key Laboratory of Hydrology-Water Resources and Hydraulic Engineering, Nanjing 210098, China

<sup>3</sup>Nanjing Hydraulic Research Institute, Nanjing 210029, China

<sup>4</sup>CSIRO, Land and Water, Private Bag 5, Wembley, WA 6913, Australia

*Correspondence to:* Guoqing Wang (gqwang@nhri.com)

10 **Abstract:** Hydrological simulations are a main method of quantifying the contribution rate (CR) of climate change (CC) and human activities (HAs) to watershed streamflow changes. However, the uncertainty of hydrological simulations is rarely considered in current research. To fill this research gap, based on the Soil and Water Assessment Tool (SWAT) model, in this study, we propose a new framework to quantify the contribution rate of climate change and human activities based on the posterior histogram distribution of hydrological simulations. In our new quantitative framework, the uncertainty of hydrological simulations is first considered to avoid the phenomenon of "equifinality for different parameters", which is common in hydrological simulations. The Lancang River (LR) Basin in China, which has been greatly affected by human activities in the past two decades, is then selected as the study area. The global gridded monthly sectoral water use data set (GMSWU), coupled with the dead capacity data of the large reservoirs within the LR basin and the Budyko hypothesis framework, are used to compare the calculation result of the novel framework. The results show that (1) the annual streamflow at Yunjinghong station in the Lancang River Basin changed abruptly in 2005, which was mainly due to the construction of the Xiaowan hydropower station that started in October 2004. The annual streamflow and annual mean temperature time series from 1961 to 2015 in the LR Basin showed a significant decreasing and increasing trend at the  $\alpha = 0.01$  significance level, respectively. The annual precipitation showed an insignificant decreasing trend. (2) The results of quantitative analysis using the new framework showed that the reason for the decrease in the streamflow at Yunjinghong station was 42.6% due to climate change, and the remaining 57.4% was due to human activities, such as the construction of hydropower stations within the study area. (3) The comparison with the other two methods showed that the contribution rate of climate change calculated by the Budyko framework and the GMSWU data were 37.2% and 42.5%, respectively, and the errors of the calculations of the new framework proposed in this study were within 5%. Therefore, the newly proposed framework, which considers the uncertainty of hydrological simulations, can accurately quantify the contribution rate of climate change and human activities to streamflow changes. (4) The quantitative results calculated by using the simulation results with the largest Nash-Sutcliffe efficiency coefficient (NSE) indicated that climate change was the dominant factor for streamflow reduction, which was in opposition to the calculation results of our new framework. In other words, our novel framework could effectively solve the calculation errors caused by the "equifinality for different parameters" of hydrological simulations. (5) The results of this case study also showed that the reduction in the streamflow in June and November was mainly caused by decreased precipitation and increased evapotranspiration, while the changes in the streamflow in other months were mainly due to human activities such as the regulation of the constructed reservoirs. In general, the novel quantitative framework

15  
20  
25  
30  
35



that considers the uncertainty of hydrological simulations presented in this study has validated an efficient alternative for quantifying the contribution rate of climate change and human activities to streamflow changes.

**Key words:** Attribution analysis; Climate change; Human activities; Lancang River Basin; Uncertainty; SWAT model

## 1. Introduction

40 Both the hydrological cycle of the watershed and water resource systems are deeply influenced by climate change (CC) and human activities (HAs) (Bao et al., 2012; Chandesris et al., 2019; Han et al., 2019; Teuling et al., 2019). Climate change mainly refers to changes in precipitation and evapotranspiration that are caused by rising temperatures and water vapor (Hegerl et al., 2015), while the impact of human activities is mainly reflected in the following aspects: reservoir construction changes the spatial and temporal distribution of streamflow processes (Hennig et al., 2013; Chandesris et al., 2019); land use changes change the characteristics of the underlying surface of the watershed, in turn affecting the streamflow of the watershed (Yang et al., 2017); 45 population increase leads to an increase in the amount of water used for domestic consumption (Teuling et al., 2019), etc. However, identifying which climate change and human activities are the main factors driving the changes in the water cycle of river basins is of great significance for water resource managers to formulate policies for sustainable water resource utilization (Dey and Mishra, 2017; Liu et al., 2017). If climate change is the dominant driving factor, then hydro-meteorologists need to assess the future trends of meteorological factors, such as precipitation and temperature, to change their water resource management strategies in a timely manner. Conversely, if human activities are the dominant factor, water resource managers should evaluate whether the impact of these human activities exceeds the local water resource carrying capacity and then adjust their related policies (Fu et al., 2004).

50 Numerous published articles have focused on how to quantify the contribution rate (CR) of climate change and human activities to the streamflow change in river basins (Bao et al., 2012; Kong et al., 2016; Chandesris et al., 2019; Han et al., 2019; Liu et al., 2019; Xie et al., 2019). In general, the commonly used methods of attribution analysis can be divided into the following three categories: 1) hydrological sensitivity and climate elasticity methods, such as the Budyko framework (Li et al., 2007; Liu et al., 2017); 2) hydrological simulation combined with scenario assumption methods (Liu et al., 2019); and 3) hydrological simulation prediction and separation methods (Han et al., 2019). What these three methods have in common is that they all need to first test the annual streamflow sequence through non-stationary testing methods (such as the Mann-Kendall test, Moving t test and LePage test, etc.), and then divide the study period into the natural period (before the break point) and the impacted period (after the break point). The first type of method needs to first calculate the sensitivity of the basin's precipitation and potential evapotranspiration to hydrological variables, and then the hydrological changes caused by climate change can be calculated combined with the hydrological sensitivity parameters through the changes in precipitation and potential evapotranspiration in the impacted period and natural period so that the CR of human activities is obtained based on the water balance equation (Li et al., 2007). The second type of method simulates multiple scenarios by changing one impact factor with other fixed factors to evaluate the contribution rate of the changed factor using lumped or distributed hydrological models (Liu et al., 2019). The core of these methods is the modelling of two situations where only one impact factor state has been changed, and the difference between the two simulation results is regarded as the influence of the changed factor. The third type of method mainly assumes that the streamflow process in the natural period is not affected by human activities, and then uses the meteorological and hydrological data in the natural period to calibrate the parameters of the hydrological model to further predict the streamflow in the impacted period. Then, the impact 70



of climate change on streamflow can be calculated by subtracting the simulated natural period streamflow from that simulated in the impacted period (Bao et al., 2012). Among the three types of methods, the third method is the most widely used because it has the following advantages: 1) relatively small data requirements (one only needs to input the meteorological and hydrological data to the hydrological model); 2) relatively simple theoretical assumptions; and 3) can quantify the CR of CC and HAs to streamflow changes at the monthly scale.

Various related published articles are briefly reviewed as follows. Bao et al. (2012) used the variable infiltration capacity (VIC) model to investigate the impacts of CC and HAs on streamflow changes in the Haihe River Basin, China, and they concluded that human activity accounted for more than 70% of the decrease in streamflow at Guantai station. Wang et al. (2013) used a two-parameter hydrological model to quantify the contribution of climate change and human activities to streamflow changes in three river basins (i.e., Zhanghe, Chaohe, and Hutuo River), and they found that human activities were the dominant factor in streamflow changes. The above literature review shows that these studies all used hydrological simulations with fixed parameter sets to quantify the impact of climate change and human activities. As pointed out by Abbaspour et al. (2004) and Zhao et al. (2018b), there is a phenomenon of "equifinality for different parameters" (Beven, 2006) in hydrological calibration and simulation, which also means that we cannot ignore the uncertainty of model parameters in the process of quantifying the CR of CC and HAs to streamflow changes because two sets of parameters with the same performance (with the same Nash-Sutcliffe efficiency coefficient) may lead to very different results; this will further influence the decision-making of water resource managers to make effective and sustainable water resource utilization policies. In the last few decades, great progress has been made in evaluating the uncertainty of hydrological simulations (Beven and Binley, 1992; Abbaspour et al., 2004; Yang et al., 2008; Zhao et al., 2018b; Farsi and Mahjouri, 2019); however, in studies related to quantifying the CR of CC and HAs for streamflow changes, few studies have considered the uncertainty of hydrological simulations (Farsi and Mahjouri, 2019). According to our literature search, Farsi and Mahjouri (2019) first considered the uncertainty of hydrological simulations in the process of quantifying the CR of CC and HAs to streamflow changes, but they only constructed the posterior distribution of the contribution rates of climate change and human activities; in their research, they did not specify how to calculate the contribution rates of CC and HAs while considering the uncertainty of hydrological simulations. Therefore, to fill this research gap, in this study we propose a new method to quantify the contribution of climate change and human activities to streamflow changes considering the uncertainty of hydrological simulations, which in summary, is developed using the posterior histogram distribution of hydrological simulations.

The Lancang River (LR) is located in southwest China, and is the largest transboundary river in the Indo-China Peninsula; it is usually called the Mekong River (MR) after flowing out of China (Grumbine and Xu, 2011). The abundant water and ecological diversity of the Lancang-Mekong River Basin nurtures tens of millions of people in many countries along the Lancang-Mekong River. The upstream flow of the river provides guarantees for irrigation and fishery water use in the countries along the MR during the dry season, and the water conservancy facilities of the LR during the peak of the flood period also provide important engineering guarantees for downstream flood control (Piman et al., 2012; Piman et al., 2016). In the past three decades, a series of hydropower stations have been constructed in the LR Basin to meet the flood control and drought relief requirements of downstream countries and the power needs of Southwest China. Therefore, it is particularly important to quantify the contribution rate of climate change and human activities to streamflow changes in the LR Basin. However, so far, there are still few corresponding studies. Han et al. (2019) chose the Lancang River Basin (LRB) as the study area and then divided the research period into three periods, the natural period, transition period, and impacted period, and combined them with the construction time of six large hydropower stations in the LR area. Finally, they found that the contribution rate of human activities during the impact



110 period exceeded 95%, using the coupled routing and excess storage (CREST) model, which was probably due to the construction  
of the Nuozhadu hydropower station. However, there are still areas for improvement in their research: 1) the results of the  
hydrological simulation were relatively poor (with monthly NSE = 0.57 for the whole study period), and 2) the uncertainty  
involved in hydrological simulations was not considered.

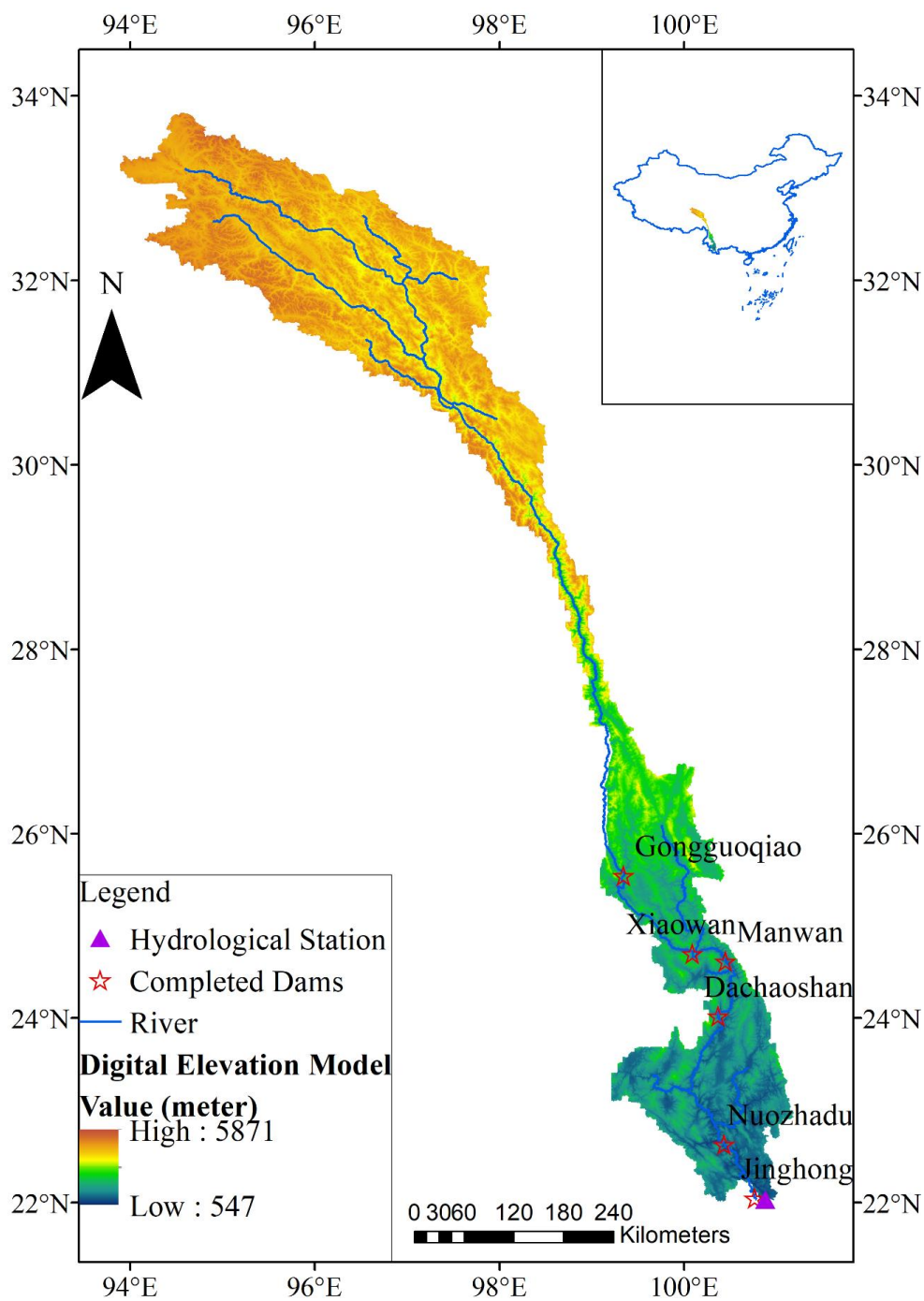
115 In this paper, the breakpoint of the change in flow regimes was identified using the Mann-Kendall break point test. Then, the  
study period was divided into a natural period (before the breakpoint) and an impacted period (after the breakpoint). The Soil and  
Water Assessment Tool (SWAT) model was used for monthly streamflow simulation at the Yunjinghong station. Next, the  
monthly SWAT model was calibrated and validated using the sequential uncertainty fitting procedure version 2 (SUFI-2)  
(Abbaspour et al., 2004). Uncertainty analysis was also conducted with the SUFI-2 method, and then the posterior histogram  
120 frequency distribution (HFD) of the CR of CC and HAs was obtained. Finally, the proposed quantification framework was  
compared with two other methods: one was the Budyko framework, and the other was to use the LR Basin's gridded monthly  
sectoral water withdrawals in the period from 1971 to 2010 (Huang et al., 2018) together with the dead reservoir storage capacity  
data of the six constructed hydropower stations along the main stream of LR, to separate the contribution rate of human activities.

## 2. Study area and data sets

### 2.1 Study area

125 The Lancang River (LR) originates in the northeastern Tanggula Mountains, Qinghai Province, China, and flows through  
China's Qinghai Province, Tibet Autonomous Region and Yunnan Province. It is the largest international river in Southeast Asia,  
and it is called the Mekong River after it flows out of China. Its main stream has a total length of ~2161 km and a total catchment  
area of ~160000 km<sup>2</sup> (Li et al., 2017a; Han et al., 2019). The topography of the LR is characterized by high northern and low  
southern portions; the maximum elevation in the northern mountainous area can reach ~5871 meters, while the lowest elevation  
130 in the downstream area is only ~547 meters (Fig. 1). This steep terrain difference also leads to the LR having a large potential for  
hydropower resources. During the past few decades, Huaneng Lancangjiang Hydropower Co., Ltd. constructed six large  
hydropower stations (i.e., Gongguoqiao, Xiaowan, Manwan, Dachaoshan, Nuozhadu and Jinghong) on the main stream of the LR  
to meet the demands for power and irrigation water in Southwest China (Fig. 1 and Table 1) (Xue et al., 2011; Hennig et al., 2013;  
Han et al., 2019). At the same time, the construction of these hydropower stations has greatly reduced the risk of flooding in  
135 downstream countries and brought great convenience to using water for downstream agricultural irrigation. Detailed information  
on the six constructed hydropower stations is outlined in Table 1. These data are mainly collected from  
<https://opendevelopmentmekong.net/topics/hydropower/>, as well as from other published related literature (Xue et al., 2011;  
Hennig et al., 2013; Tilt and Gerkey, 2016; Han et al., 2019).

140 The LR features an arid climate in the upper mountainous areas, while the lower reaches are dominated by humid climates. The  
average annual precipitation of the whole basin is ~ 870 mm based on a 55-year record (from 1961 to 2015) using the China  
Gauge-based Daily Precipitation Analysis (CGDPA) (Xie et al., 2007; Tang et al., 2019). Due to the influence of the westerlies  
and the Indian Ocean monsoon, the precipitation in the LR has obvious seasonal changes, and the precipitation from June to  
September accounts for more than 70% of the annual precipitation (Jacobs, 2002). Correspondingly, the streamflow of the LR  
also shows seasonality, and the floods are mostly concentrated from June to September.



145

**Fig. 1.** Locations of the Lancang River (LR) Basin, Yunjinghong hydrological station, constructed dams on the main stream of the LRB, and main rivers and elevations (m).



150

**Table 1** Basic information for the six large constructed dams on the mainstream of the Lancang River

Hydropower station	Manwan	Dachaoshan	Jinghong	Xiaowan	Gongguoqiao	Nuozhadu
Date of river closure	1987.12	1997.11	2005.01	2004.10	2008.12	2007.11
Date of complete construction	1995.06	2003.10	2009.05	2010.08	2012.03	2014.06
Drainage area (10 <sup>4</sup> km <sup>2</sup> )	11.45	12.10	14.91	11.33	9.73	14.47
Dead reservoir storage (km <sup>3</sup> )	0.668	0.371	0.81	4.35	0.316	10.3
Total reservoir storage (km <sup>3</sup> )	0.92	0.94	1.40	15.3	0.365	22.7
Installed capacity (10 <sup>4</sup> kw)	150	135	150	420	90	500

(Notation: Dead storage capacity refers to the storage capacity below the dead water level of the reservoir, which does not participate in runoff regulation during the normal operation of the reservoir.)

## 2.2 Data sets

155 The China Gauge-based Daily Precipitation Analysis (CGDPA) product was developed by the China Meteorological Administration (CMA) using data from ~2400 ground-based national weather stations across China (Xie et al., 2007; Shen et al., 2014; Tang et al., 2018). It provides daily precipitation, maximum temperature, minimum temperature, relative humidity, and wind speed data at a 0.25-degree spatial resolution from 1961 to 2015 (<http://cdc.nmic.cn>). Previous studies have successfully applied this product to multiple research areas in China (Tang et al., 2018; Han et al., 2019; Tang et al., 2019). The daily streamflow data from Yunjinghong station for the time period from 1961 to 2015 were collected from the Information Center of the Ministry of Water Resources and the local water resources management department.

160 The digital elevation model (DEM) used in this study was downloaded from NASA's Shuttle Radar Topography Mission (SRTM) data bank at a spatial resolution of ~90 meters (<http://srtm.csi.cgiar.org/>), which was used to generate the watershed boundary, slope and sub-watershed data in the SWAT model (Arnold et al., 2012a). The Harmonized World Soil Database (version 1.2) (HWSD v1.2) at a spatial resolution of ~1 km was downloaded from the Food and Agriculture Organization of the United Nations, and this data set contains two layers of soil. The land use and cover data with a spatial resolution of ~1km were collected from the Geospatial Data Cloud (<http://www.gscloud.cn/>). In this study, to analyze the land use change in the LR during the historical period, we collected five periods of land use data in the 1980s, 1990s, 2000s, and from 2010 to 2015.

170 The global gridded monthly sectoral water use (GMSWU) data set for 1971-2010 was obtained from <https://zenodo.org/record/1209296#.XsJmiTNIsSJ>. This data set was developed by Huang et al. (2018), and it provides the global domestic water use, irrigation water use, livestock water use, manufacturing water use and mining water use with a spatial resolution of 0.5 degrees. We used this data set here to roughly separate the effects of human activities in the LR. For more technical information about this set of products, the readers can refer to Huang et al. (2018) and Han et al. (2019). Furthermore, detailed information on six large dams in the main stream of the LR was collected from Open Development Mekong (<https://opendevelopmentmekong.net/topics/hydropower/>) and Huaneng Lancang River Hydropower Inc. It mainly includes the dates when the rivers start to be closed, when these dams were fully put into use, their dead storage capacity, their total storage capacity, and other information.

175



### 3. Methodologies

#### 3.1 The novel proposed framework

Hydrological simulation is one of the main methodologies to quantify the contribution rate of climate change and human activities to streamflow variations; however, in the past, related studies have rarely considered the uncertainty involved in hydrological simulations (Farsi and Mahjouri, 2019). In this section, we will introduce a new quantitative framework to avoid the common phenomenon of "equifinality for different parameters" in hydrological simulation, by constructing the posterior distribution of streamflow simulations during the implementation process. The specific implementation flowchart is shown in Fig. 2. The detailed execution steps are shown as follows.

Step 1: Inspection of break points in the annual streamflow sequence; based on the result of break point test, the entire time series is divided into a natural period (before the break point) and an impacted period (after the break point).

Step 2: Sensitivity analysis of the parameters in the hydrological model.

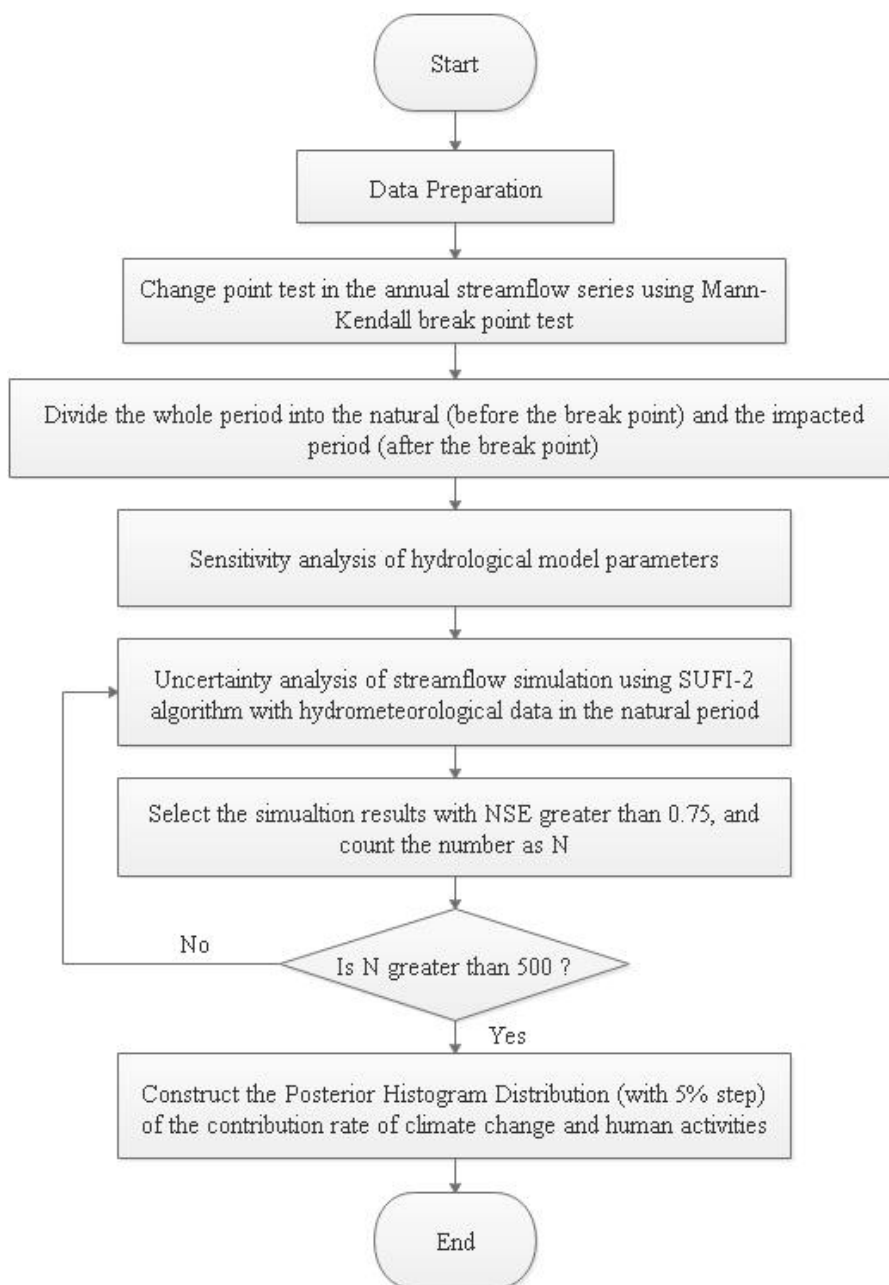
Step 3: According to the results of the parameter sensitivity analysis, selection of the more sensitive parameters and input of the hydrometeorological data of the natural period to calibrate the hydrological model with 1000 runs.

Step 4: Selection of the parameter sets with Nash-Sutcliffe efficiency coefficients (NSE) is greater than 0.75 in 1000 simulations, input of the hydrometeorological data of the impacted period, and further calculation of the CR of CC and HAs to the streamflow change corresponding to each simulation result.

Step 5: Construction of the posterior histogram distribution (PHD) of the CR of CC and HAs (with a 5% step), and then the histogram with the highest frequency is treated as the uncertainty contribution rate interval of CC and HAs to the streamflow change.

Step 6: The arithmetic mean of the results in the interval is treated as its true contribution rate.

In step 4, to ensure the number of streamflow simulation samples, we set the simulation results with NSE is greater than 0.75 to at least 500 times. If the setting is not met, then step 3 is repeated until the cumulative simulation times are greater than 500 times.



200

**Fig. 2.** Flowchart of the newly proposed quantitative framework.

### 3.2 Mann-Kendall test

In this step, the trends and break points of the hydrometeorological data are detected using the nonparametric Mann-Kendall monotonic trend test (Mann, 1945; Kendall, 1975; Gilbert, 1987) and the Mann-Kendall break point test (Sneyers, 1991),



205 respectively. The main consideration of using the Mann-Kendall test is that this method assumes no particular distribution for the  
 tested time series (Xu et al., 2018; Song et al., 2019). Significance levels of  $\alpha = 0.01$  and  $0.05$  is used in this study.

### 3.2.1 Mann-Kendall monotonic trend test

210 The Mann-Kendall (MK) monotonic trend test was developed by Mann (1945), Kendall (1975) and Gilbert (1987), which  
 has been widely used to detect the presence of an upward or downward trend of the hydrometeorological time series, and the  
 advantage of this test is that the time series does not need to follow a certain distribution (Hamed and Ramachandra Rao, 1998).  
 This method first tests whether to reject the null hypothesis ( $H_0$ : no monotonic trend) and accept the alternative hypothesis ( $H_a$ :  
 with monotonic trend) for a significance level of  $\alpha$ . The defined statistic  $S$  can be calculated by the following equation:

$$S = \sum_{k=1}^{n-1} \sum_{j=k+1}^n \text{sign}(x_j - x_k) \quad (1)$$

where  $x_k$  is the data in the order over time,  $x_1, x_2, \dots, x_{n-1}$ , which means the time series obtained at times  $1, 2, \dots, n-1$ , respectively;  
 215  $x_j$  is another time series over time  $x_{k+1}, x_{k+2}, \dots, x_n$ ;  $n$  is the length of the data set record; and  $\text{sign}(x_j - x_k)$  is a sign function  
 that takes on the values of  $1, 0$ , or  $-1$  based on the sign of  $x_j - x_k$ , and its values can be calculated by the following equation:

$$\text{sign}(x_j - x_k) = \begin{cases} -1, & x_j - x_k < 0 \\ 0, & x_j - x_k = 0 \\ 1, & x_j - x_k > 0 \end{cases} \quad (2)$$

After calculating the  $S$  sequence, the variance of  $S$  can be computed as follows:

$$\text{VAR}(S) = \frac{1}{18} \left[ n(n-1)(2n+5) - \sum_{p=1}^g t_p(t_p-1)(2t_p+5) \right] \quad (3)$$

220 where  $n$  is the length of the time series;  $g$  is the length of any given tied group and  $t_p$  is the length of the data set series in the  
 $p_{th}$  group. Then, the defined test statistic  $Z_{MK}$  can be transformed from the statistical value  $S$ , and the equation is as follows:

$$Z_{MK} = \begin{cases} = \frac{S-1}{\sqrt{\text{VAR}(S)}} & \text{if } S > 0 \\ = 0 & \text{if } S = 0 \\ = \frac{S+1}{\sqrt{\text{VAR}(S)}} & \text{if } S < 0 \end{cases} \quad (4)$$

At the given significance level  $\alpha$ , if  $-Z_{\alpha/2} \leq Z_{MK} \leq Z_{\alpha/2}$ , then the  $H_0$  (null hypothesis) is accepted, which means that  
 there is no significant trend in the time series. By contrast, a positive  $Z_{MK}$  indicates that the tested time series has an upward trend,  
 225 while a negative value indicates a downward trend.



### 3.2.2 Mann-Kendall break point test

The break point of the hydrometeorological time series denotes a change from one stable state to another stable state (Xu et al., 2018). It occurs when the climate system breaks through a certain threshold. The Mann-Kendall break point test has been widely used to test break points for hydrometeorological time series, signaling when abrupt changes start (Sneyers, 1991). This test method is used to determine the break point of the observed annual streamflow in this study. The defined statistic  $UF_k$  is obtained by the following formulas:

$$UF_k = \frac{S_k - E(S_k)}{\sqrt{Var(S_k)}} \quad k = 1, 2, \dots, n \quad (5)$$

$$S_k = \sum_{i=1}^k r_i \quad r_i = \begin{cases} 1 & x_i > x_j \\ 0 & else \end{cases} \quad j = 1, 2, \dots, i \quad (6)$$

where  $x_i$  is the variable to be tested and  $n$  is the total number of data points. The expectation  $E(S_k)$  and variance  $Var(S_k)$  of the data series can be calculated as follows:

$$E(S_k) = \frac{n(n-1)}{4} \quad (7)$$

$$Var(S_k) = \frac{n(n-1)(2n+5)}{72} \quad (8)$$

$UF_k$  is a sequence of statistics calculated by arranging  $x_1, x_2, \dots, x_n$  in the order of time series  $x$  that obeys the standard normal distribution. Then, treating the time series  $x$  in reverse order  $x_n, x_{n-1}, \dots, x_1$ , the above process is repeated, but by using a reversed definition of  $UB_k = -UF_k, k = n, n-1, \dots, 1$ . Given the significance level  $\alpha$  (0.01 in this study), if  $UB_k = -UF_k, k = 1, 2, \dots, n$ , no significant trend is detected, where  $U_{\alpha/2}$  is the standard normal deviation. In contrast, this means that the tested sequence has a significant upward or downward trend when  $|UF_k| > U_{\alpha/2}$ . Then, the curves of  $UF_k$  and  $UB_k$  are plotted. If there is an intersection of the two curves and the trend of the data series is statistically significant, then this intersection is regarded as the break point of the data series.

After identification of the break points in the annual streamflow series, the study period is divided into a “natural period” (before the break point) and an “impacted period” (after the break point) (Bao et al., 2012; Wang et al., 2015). The “natural period” means that there is no significant increase or decrease in streamflow during this period, and it also means that relatively slow climate change is the dominant factor, and that the impact of human activities is very small during this period. Consequently, the impacted period indicates a significant change in streamflow during this period, mostly due to factors such as the construction of water conservancy engineering facilities, increased water consumption for irrigation, changes in land use and increased water consumption in cities and towns.



### 3.3 SWAT model

The Soil & Water Assessment Tool (SWAT) model is a semi-distributed, physical process-based hydrological model developed by the Agricultural Research Service of the United States Department of Agriculture (USDA-ARS) (Arnold et al., 1998). The SWAT model first divides the study area into several subbasins based on DEM data, and then each subbasin is further divided into several HRUs (Hydrologic Response Units) based on land use and soil data sets. Then, streamflow generation at the subbasin scale is calculated following the principles of water balance and energy balance after inputting the meteorological data sets. Finally, the total flow of river basin exports is calculated according to the Muskingum method (Arnold et al., 2012b; Tang et al., 2019). We chose to use the SWAT model in this study because numerous published studies have proven that this model has excellent performance in hydrological simulations across the world (Lee et al., 2018; Zhao et al., 2018a; Zhao et al., 2018b; Tang et al., 2019).

The calibration of model parameters is executed using the independent software SWAT-CUP, which was developed by Abbaspour et al. (2007). This software is freely available and provides five parameter calibration and uncertainty analysis methods. In this study, the sequential uncertainty domain parameter fitting version 2 (SUFI-2) algorithm (Abbaspour et al., 1997; Abbaspour et al., 2004) was used to perform parameter calibration and uncertainty analysis, because this method has proven to have the advantages of shorter calculation time, ease of implementation and ability to set arbitrary objective functions (Wu and Chen, 2015; Tuo et al., 2016; Zhao et al., 2018b). The performance of the SWAT model was evaluated by the Nash-Sutcliffe efficiency coefficient (NSE) (Nash and Sutcliffe, 1970) and relative error (RE):

$$NSE = 1 - \frac{\sum_{i=1}^N (Q_{obs,i} - Q_{sim,i})^2}{\sum_{i=1}^N (Q_{obs,i} - \overline{Q_{obs}})^2} \quad (9)$$

$$RE = \frac{R_{sim} - R_{obs}}{R_{obs}} \times 100\% \quad (10)$$

where  $Q_{obs,i}$  and  $Q_{sim,i}$  are the observed and simulated streamflow, respectively;  $\overline{Q_{obs}}$  is the mean value of the observed streamflow;  $N$  is the total number of days or months in the calibration period; and  $R_{sim}$  and  $R_{obs}$  are the mean annual simulated and observed streamflow, respectively.

### 3.4 Construction of the Posterior Histogram Distribution of contribution rate

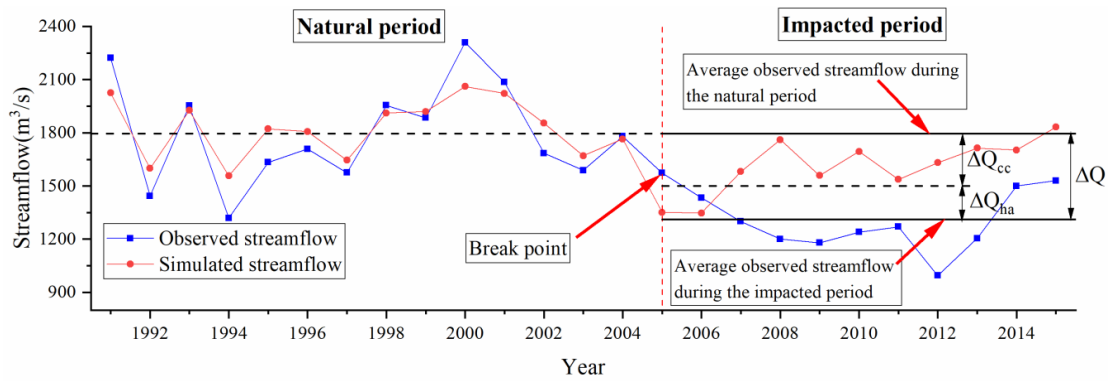
In this section, we introduce how to calculate the contribution rate (CR) of climate change (CC) and human activities (HAs) to streamflow variations and how to construct the posterior histogram distribution (PHD) of the CR to consider the uncertainty of hydrological simulations.

#### 3.4.1 Contribution rate of climate change and human activities

A schematic diagram of the attribution evaluation of streamflow changes is shown in Fig. 3.  $\Delta Q$  in the figure represents the amount of change in the observed streamflow during the impacted period based on the natural period, while  $\Delta Q_{cc}$  and  $\Delta Q_{ha}$  represent the amount of streamflow change caused by climate change and human activities, respectively. The total change in the annual streamflow can be calculated using the following formula:

$$\Delta Q = \Delta Q_{cc} + \Delta Q_{ha} = \overline{Q_{oi}} - \overline{Q_{on}} \quad (11)$$

where  $\overline{Q_{oi}}$  and  $\overline{Q_{on}}$  are the mean annual observed streamflow ( $m^3/s$ ) in the impacted period and natural period, respectively.



285

**Fig. 3.** Schematic diagram of the contribution rate of climate change (CC) and human activities (HAs) to streamflow change using SWAT modelling. (Notation:  $\Delta Q$ ,  $\Delta Q_{cc}$  and  $\Delta Q_{ha}$  respectively represent the amount of streamflow change in the impacted period, the amount of streamflow change caused by climate change, and the amount of streamflow change caused by human activities.)

290

The hydrological and meteorological data in the natural period are input into the SWAT model, and using the SUFI-2 method to calibrate the model, a set of parameters represents the characteristics of catchment under natural conditions with less impact from human activities. Then, this set of parameters is brought back into the SWAT model using the meteorological data of the impacted period. Based on the above simulation results, the climate change induced in streamflow can be calculated as follows:

$$\Delta Q_{cc} = \overline{Q_{st}} - \overline{Q_{sn}} \quad (12)$$

295

where  $\overline{Q_{st}}$  and  $\overline{Q_{sn}}$  represent the mean simulated annual streamflow ( $m^3/s$ ) for the impacted period and natural period, respectively. Thus, the streamflow change induced by human activities can be calculated by the following equation:

$$\Delta Q_{ha} = \Delta Q - \Delta Q_{cc} \quad (13)$$

After the calculation of  $\Delta Q_{cc}$  and  $\Delta Q_{ha}$ , the contribution rate of climate change and human activities to streamflow changes, which are defined as  $CR_{cc}$  and  $CR_{ha}$ , respectively, can be estimated as:

300

$$CR_{cc} = \frac{|\Delta Q_{cc}|}{|\Delta Q|} \times 100\% \quad (14)$$

$$CR_{ha} = \frac{|\Delta Q_{ha}|}{|\Delta Q|} \times 100\% \quad (15)$$

Equations 12 to 15 are also applicable to quantify the contribution rate of climate change and human activities to streamflow changes on a monthly scale.

### 3.4.2 Construction of the PHD of the CR of CC and HAs

305

Before the construction of the PHD of the CR of CC and HAs, the sensitivity of the parameters of the SWAT model is first conducted. Based on the related published literature (Yang et al., 2008; Malagò et al., 2015; Zhao et al., 2018b) and the authors' experience, the Latin-Hypercube and global sensitivity methods were used to perform the uncertainty analysis (Abbaspour et al., 2007). The global sensitivity analysis method is the estimation of the average change in the objective function caused by the change in each parameter, and all parameters change during the whole process. A t-test was used to identify the relative sensitivity



310 of each parameter. Considering the influence of the snowmelt streamflow process upstream of the LR Basin on the hydrological simulation, 22 parameters were selected and the details of these selected parameters are shown in Table 2. According to the suggestion of Abbaspour et al. (2004), 500 simulations were set up to implement the sensitivity analysis. The t-stat and P-values were used to measure which parameters were more sensitive, where a larger absolute t-stat value and a smaller absolute P-value represent a higher sensitivity of a given parameter.

315 **Table 2** Twenty-two selected SWAT model parameters in the sensitivity analysis at Yunjinghong station

Parameter	Description	Parameter Range
R_CN2	SCS runoff curve number for soil condition II	-0.2 – 0.2
R_SOL_AWC	Available water capacity of each soil layer	-0.2 – 0.1
A_GWQMN	Threshold depth of water in the shallow aquifer required for return flow to occur	0 – 25
V_SNOCOVMX	Minimum snow water content that corresponds to 100% snow cover	0 – 500
V_SMFMN	Minimum melt rate for snow during the year (occurs on the winter solstice)	0 – 20
V_CH_K2	Effective hydraulic conductivity in the main channel alluvium	0 – 500
V_GW_REVAP	Groundwater "revap" coefficient	0.02 – 0.2
V_REVAPMN	Threshold depth of water in the shallow aquifer for "revap" to occur	0 – 500
V_GW_DELAY	Groundwater delay (days)	0 – 500
V_ALPHA_BF	Baseflow alpha factor (days)	0 – 1
V_SOL_BD	Moist bulk density	0.9 – 2.5
A_ESCO	Soil evaporation compensation factor	0 – 0.2
V_OV_N	Manning's "n" value for overland flow	-0.01 – 0.6
R_RCHRG_DP	Deep aquifer percolation fraction	0 – 1
V_CH_N2	Manning's "n" value for the main channel	0.018 – 0.15
R_SLSUBBSN	Average slope length	0 – 0.2
V_SMTMP	Snowmelt base temperature	-5 – 5
V_TLAPS	Temperature lapse rate	-10 – 10
V_SMFMX	Maximum melt rate for snow during year	0 – 20
R_SOL_K	Saturated hydraulic conductivity	-0.8 – 0.8
V_SFTMP	Snowfall temperature	-5 – 5
V_ALPHA_BNK	Baseflow alpha factor for bank storage	0 – 1

(Notation: R\_, V\_, and A\_ represent multiplying, replacing, and adding the corresponding parameter values, respectively, in the process of calibrating the parameters.)

320 Based on the sensitivity analysis results, 9 parameters with the highest sensitivity were selected to re-calibrate the model with 1000 simulations. According to the recommendations in Tuo et al. (2016) and Moriasi et al. (2007), the performance of the hydrological simulation can be divided into four grades based on the NSE values: very good performance ( $0.75 \leq NSE < 1$ ), good performance ( $0.65 \leq NSE < 0.75$ ), satisfactory performance ( $0.5 \leq NSE < 0.65$ ) and unsatisfactory performance ( $NSE < 0.5$ ). According to this evaluation standard, we selected simulation results with NSE greater than 0.75 out of 1000 simulation results to construct the posterior histogram frequency distribution (PHD) of the contribution rate of climate change and human activities to



streamflow changes using the method introduced in section 3.4.1. Note that to reduce the random error caused by the number of  
 325 samples, we set the number of simulations with NSEs  $\geq 0.75$  to be more than 500; that is, we needed to repeatedly use Latin  
 hypercube sampling and the SUFI-2 algorithm until the number of simulation results that met the conditions was more than 500.  
 Then, the CR of more than 500 groups of CC and HAs to streamflow change was calculated. Finally, the posterior histogram  
 distribution (PHD) of the CR of CC and HAs was constructed in 5% steps. At this stage, the histogram column with the highest  
 frequency in the PHD was selected as the result of quantitative analysis, which considered the uncertainty, and the arithmetic  
 330 average of all results in the column was used as the actual value of the CR of climate change and human activities.

### 3.5 Comparison of the newly developed quantification method with other two methods

In order to evaluate the calculation accuracy of the novel framework proposed in this study to quantify the CR of CC and HAs  
 to streamflow changes, the Budyko framework was used first. This framework was developed by Budyko (1961) and links climate  
 variability to streamflow ( $Q$ ) and actual evapotranspiration ( $AE$ ) through the assumption that the long-term average annual  
 335 catchment  $AE$  is determined by the catchment average precipitation ( $P$ ) and the catchment potential evapotranspiration ( $PET$ ) (Liu  
 and Liang, 2015). Over the past few decades, the Budyko framework and its variants have been widely used to conduct climate  
 change and human activity attribution analyses of streamflow changes (Liu et al., 2017; Han et al., 2019; Xin et al., 2019).  
 According to its theoretical assumptions, the multiyear average water balance within the catchment can be expressed as follows:

$$\Delta S = P - AE - Q \quad (16)$$

340 where  $P$ ,  $Q$ , and  $AE$  represent the multiyear average precipitation (mm), streamflow (mm) and actual evapotranspiration (mm),  
 respectively;  $\Delta S$  (mm) is the change in the amount of water storage at the watershed scale, and it is reasonable to assume that it is  
 equal to 0 on the multiyear average scale. According to Zhang et al. (2001), the  $AE$  can be calculated by the following formula:

$$\frac{AE}{P} = \frac{1 + \omega(PET/P)}{1 + \omega(PET/P) + (PET/P)^{-1}} \quad (17)$$

345 where  $\omega$  is the plant-available water coefficient which is related to the vegetation type of the catchment; it is set to 0.5 in this  
 study.

The changes in the catchment streamflow due to climate change, which are mainly characterized by precipitation ( $P$ ) and actual  
 evapotranspiration ( $AE$ ), can be expressed as follows:

$$\Delta Q_{cc} = \alpha \Delta P + \beta \Delta AE \quad (18)$$

350 where  $\Delta Q_{cc}$  (mm) represents the streamflow changes induced by climate change;  $\alpha$  and  $\beta$  represent the sensitivity of streamflow  
 to precipitation and actual evapotranspiration, respectively; and  $\Delta P$  and  $\Delta AE$  are the changes in precipitation and actual  
 evapotranspiration in the impacted period compared to the natural period, respectively. The sensitivity coefficients  $\alpha$  and  $\beta$   
 are defined as follows:

$$\alpha = \frac{1 + 2DI + 3\omega DI}{(1 + DI + \omega(DI)^2)^2} \quad (19)$$

$$\beta = -\frac{1 + 2\omega DI}{(1 + DI + \omega(DI)^2)^2} \quad (20)$$

355 where  $DI$  is the dryness index which is equal to  $PET/P$ .

Through the above formulas, we can separate the contribution rate of climate change to streamflow variations, and further  
 compare it with the calculation results of the new method proposed in this paper.



In addition to the Budyko framework, we also used the GMSWU data introduced in Section 2.2 and the reservoir dead storage capacity data to roughly separate the CR of HAs from the streamflow changes in the LR Basin. The GMSWU data set provides five types of water withdrawals (i.e., irrigation, livestock, domestic use, mining, and manufacturing) within the period of 1970 to 2010 in the LR Basin, and it was generated by downscaling country-scale estimates of different sectoral water withdrawals from the Food and Agriculture Organization (FAO) of the United Nations AQUASTAT, which ensured its good accuracy (Huang et al., 2018). Here, AQUASTAT refers to FAO's Global Information System on Water and Agriculture (<http://www.fao.org/aquastat/en/>). Catchment-scale annual water use data were calculated by spatially averaging all grids within the LR Basin, and then streamflow changes caused by each type of water use were obtained using the average annual water use value during the impacted period minus that during the natural period. As shown by Han et al. (2019) and Zhao et al. (2012), during the past two decades, dam construction has been the most significant human activity affecting the streamflow changes in the LR Basin. Therefore, in this study, we converted the dead storage capacity of 6 large reservoirs (Table 1) into units of millimeters according to their watershed control area because the impact of the reservoir on the outlet flow of the watershed can be used as its minimum impact value on the multiyear average scale. Note that the CR of CC and HAs calculated by the above two methods was not the actual true value but rather an estimate. We used these two methods to compare with the newly proposed framework developed in this study. In addition, although the calculations of these two methods are simple, they have the following shortcomings compared with the CR of CC and HAs derived from hydrological simulation: 1) the CR of CC and HAs to streamflow variations can only be calculated on a multiyear average scale and cannot be calculated on a monthly or seasonal scale; 2) they have higher requirements for data input (e. g., data related to reservoirs); and 3) they have relatively less physical meaning compared with the streamflow simulation of the distributed hydrological model.

## 4. Results

### 4.1 Hydrological and Meteorological trends in the LR Basin

#### 4.1.1 Trends and break points of the streamflow

The results of the Mann-Kendall break point test for the annual streamflow at Yunjinghong station within the period from 1961 to 2015 are shown in Fig. 4. Since the intersection of the UF and UB curves in Fig. 4 is within the confidence intervals (of 0.05 and 0.01), the break point of the annual streamflow in the LR Basin occurred in 2005. Combined with the construction of reservoirs in the LR Basin, the construction of the Xiaowan hydropower station started in October 2004 (with total storage capacity = 15.3 km<sup>3</sup>). Therefore, according to the principle of time division introduced in Section 3.1, the study period can be divided into the natural period (from 1961 to 2004) and the impacted period (from 2005 to 2015). UF curves of the MK break point test represent the trend of the time series. As shown in Fig. 4, the observed annual streamflow at Yunjinghong station had an increasing trend before 1967, after which the annual streamflow experienced a significant decreasing trend until 2015.

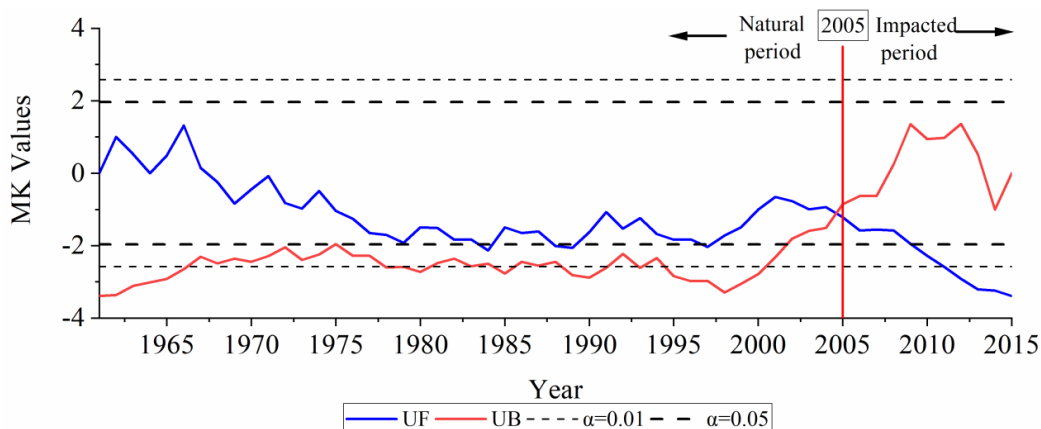


**Fig. 4.** The Mann-Kendall break point testing statistics of the annual streamflow for the Lancang River Basin from 1961 to 2015.

390 Fig. 5 shows the MK monotonic trend testing statistics of the annual and monthly streamflow for the LR Basin from 1961 to 2015. A positive Z statistic represents an upward trend in the time series, and vice versa. The annual average streamflow in the LR Basin showed a significant decreasing trend, and passed the 0.01 significance level. This decreasing trend of the annual streamflow in the LR Basin is consistent with the conclusions of Han et al. (2019). For the monthly streamflow, the streamflow from February to May showed an increasing trend, among which March and May passed the significance level of 0.05 (with the Z statistic greater than 1.96). The streamflow in the remaining months showed a decreasing trend. Except for June, the decreases in the other months all passed the 0.05 significance level. The decrease in the streamflow from August to October even passed the 0.01 significance test. Among them, the largest decrease was in August (Z statistic = -4.23). This trend of changes in streamflow during the year was mainly caused by the operation of reservoirs within the basin, because reservoirs often release flows during dry periods (from January to May) to alleviate possible droughts in the downstream areas, and they store water during wet periods (from June to October) to reduce the flood control pressure in the downstream area below the reservoir.

395  
400

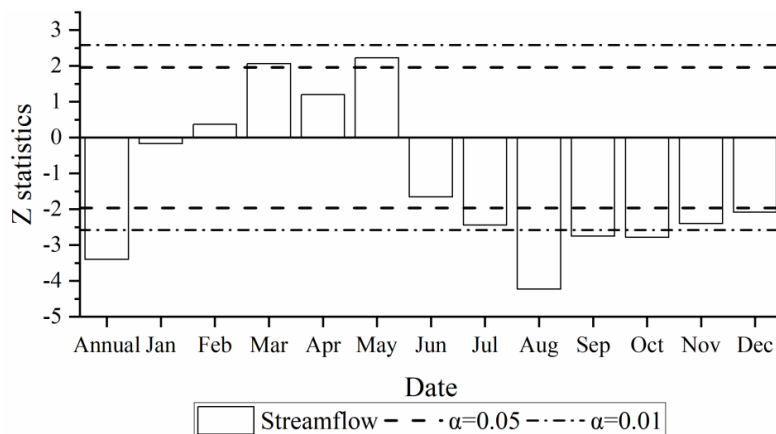


**Fig. 5.** The Mann-Kendall monotonic trend test statistics of the annual and monthly streamflow for the Lancang River Basin from 1961 to 2015.



#### 4.1.2 Trends and break points of the mean areal precipitation and temperature

405 The time series and MK break point test results of the annual areal precipitation and mean temperature for the LR Basin from 1961 to 2015 are presented in Fig. 6. In general, changes in the annual precipitation were more complicated than changes in the mean temperature in the LR Basin. The precipitation showed a fluctuating trend, while the mean temperature almost showed a continuous rising trend throughout the study period.

410 As shown by the time series of the annual precipitation in the LR Basin in Fig. 6 (a), there was a slightly decreasing trend in the LRB during the last 55 years, especially in the past 10 years, but this trend was not significant according to the result of the MK test at the  $\alpha = 0.05$  significance level. The areal annual precipitation in 1985 reached 971 mm, which was the highest in the last 55 years. In 2009, it was 769 mm, which was the lowest value from 1961 to 2015. The MK break point test results showed that there were 11 break points in the annual precipitation time series. Regarding the positive and negative changes in the UF value, the annual precipitation showed a fluctuating trend from 1961 to 1966; then until 1998, the annual precipitation showed a small decreasing trend (except in 1991); from 1999 to 2006, the annual precipitation experienced a small increase; and in the last 9 years (2007-2015), the annual precipitation in the study area showed a decreasing trend.

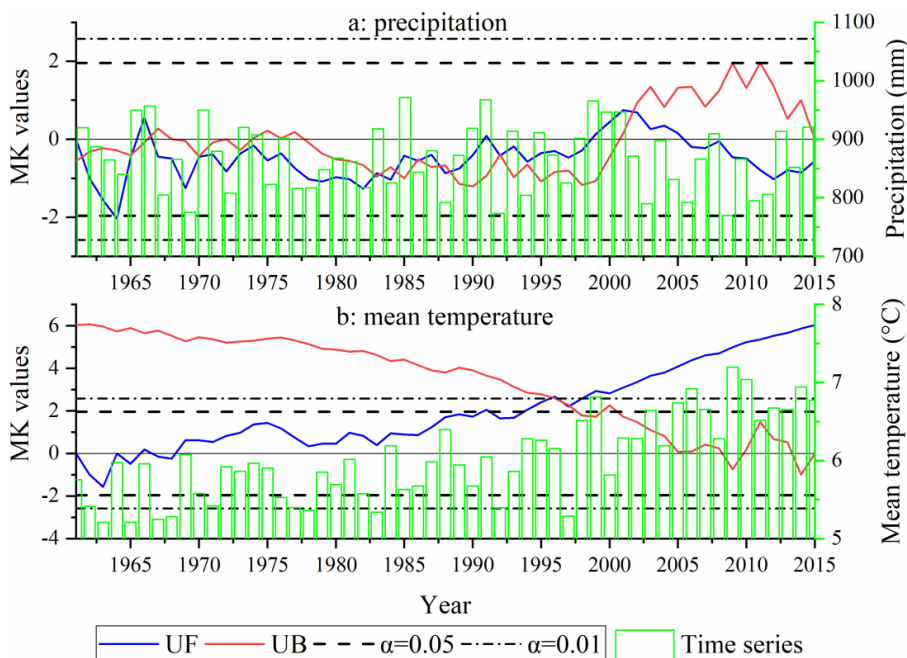


**Fig. 6.** Time series and the Mann-Kendall break point test statistics of the annual precipitation (a) and mean temperature (b) in the Lancang River Basin from 1961 to 2015.

420 The time series of the annual mean temperature in the LR Basin presented in Fig. 6 (b) shows that the annual mean temperature in the study area changed relatively smoothly before 1998. After 1998, the temperature began to rise significantly and exceeded the significance level of 0.01. The annual mean temperature in 1963 reached 5.2 °C, the coldest temperature in the study period. The hottest year was 2009, during which the mean temperature was 7.2 °C. In terms of changes in the UF value, the mean temperature showed a fluctuating trend from 1961 to 1968, and then continued to rise until it exceeded the significance level



425 of 0.05 in 1991 and exceeded the significance level of 0.01 in 1998. The break point of the annual mean temperature was detected in 1997.

The MK monotonic trend test statistics of the annual and monthly precipitation and mean temperature for the LR Basin from 1961 to 2015 are presented in Fig. 7. The annual precipitation in the study area showed an insignificant decreasing trend (Z statistic = -0.55), while the annual average temperature showed a significant increasing trend (Z statistic = 6.02) and exceeded the significance level of 0.01. The monthly change in precipitation also showed a fluctuating trend. The increasing trend of precipitation in April and the decreasing trend of precipitation in June exceeded the significance level of 0.05, while the trends of precipitation in other months were not significant ( $|z \text{ statistic}| < 1.96$ ). The trend of the monthly mean temperature was relatively simple. Except for the increase in the mean temperature in November, which passed the significance level of 0.05, the increasing trend of the mean temperature in all other months passed the significance level test of 0.01. This also means that the climate in the study area has been gradually warming and drying during the past 55 years.

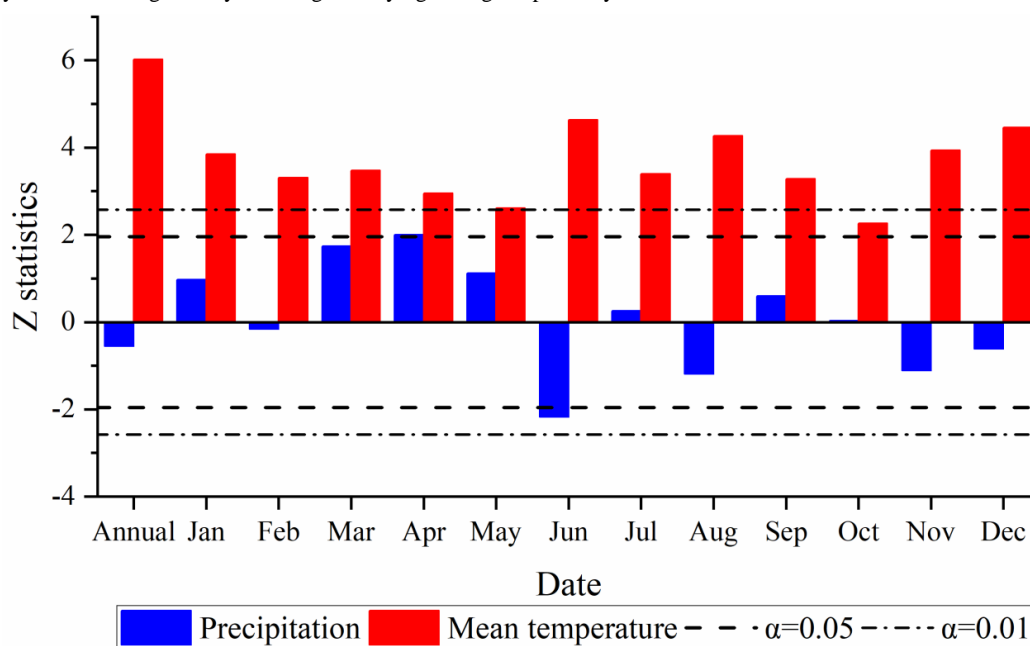


Fig. 7. The Mann-Kendall monotonic trend test statistics of the annual and monthly precipitation and mean temperature for the Lancang River Basin from 1961 to 2015.

## 4.2 Results of the SWAT simulations

### 4.2.1 Sensitivity analysis of the SWAT model parameters

As described in Section 3.4.2, the sensitivity of 22 selected parameters was evaluated using the SUFI-2 and global sensitivity analysis methods. SUFI-2 performs a combined optimization and uncertainty analysis using a global search procedure and can deal with a large number of parameters through Latin hypercube sampling. The sensitivity evaluation indexes, the t-Stat and P-value, of 22 parameters are shown in Table 3. Obviously, the sensitivity ranks of the parameters calculated based on SUFI-2



445 showed that ALPHA\_BNK has the highest sensitivity, followed by CH\_K2, SOL\_BD, GW\_REVAP, SFTMP, CN2, SOL\_K, SMTMP and ALPHA\_BF, whereas the other 14 parameters have less sensitivity for the streamflow simulation. ALPHA\_BNK mainly controls the baseflow process within the watershed, and this parameter has also proven to have high sensitivity in other relevant studies (Wu and Chen, 2015), especially in mountainous areas. CH\_K2 and ALPHA\_BF are mainly related to groundwater runoff, CN2 is the SCS runoff curve number, and these parameters all have higher sensitivity in many published  
 450 articles on the SWAT model parameter sensitivity (Wu and Chen, 2015; Zhao et al., 2018b). Other parameters with high sensitivity, such as SFTMP and SMTMP, which mainly control the snowmelt process in the basin, also indicate that snowmelt runoff plays an important role in the recharge of the LR Basin (Gao et al., 2019). Based on the above sensitivity analysis results, the top 9 parameters of the sensitivity ranking were selected for further research.

**Table 3** Basin wide sensitivity ranking calculated from 22 selected parameters using SUFI-2

Parameter	t-Stat	P-Value	Parameter	t-Stat	P-Value
V_ALPHA_BNK	38.1	0	V_CH_N2	1.25	0.21
V_CH_K2	-10.5	0	V_TLAPS	1.19	0.23
V_SOL_BD	6.81	0	A_ESCO	1.12	0.24
V_GW_REVAP	-5.0	0	V_SNOCOVMX	-1.01	0.31
V_SFTMP	-4.73	0	V_PLAPS	-0.73	0.47
R_CN2	4.60	0	V_GW_DELAY	-0.68	0.50
R_SOL_K	4.34	0	R_SLSUBBASN	-0.65	0.52
V_SMTMP	3.41	0	V_OV_N	0.44	0.66
V_ALPHA_BF	-2.70	0	V_SMFMX	0.36	0.72
R_SOL_AWC	-2.46	0.01	A_GWQMN	0.15	0.88
R_RCHRG_DP	-1.74	0.08	V_REVAPMN	-0.07	0.94

455 (Notation: V\_ represents replacing the default value with the given value; R\_ represents the relative change (%); and A\_ represents adding the given value to the original parameter value)

#### 4.2.2 Results of the SWAT simulations

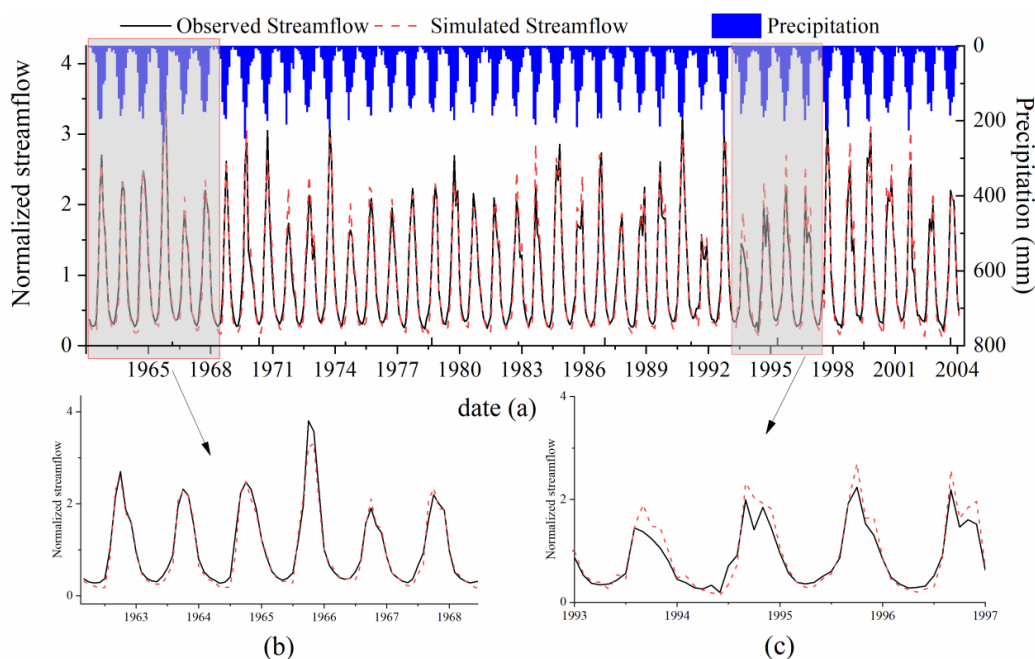
As mentioned above, the 9 parameters with the highest sensitivity rankings that controlled different stages of the basin's streamflow production and flow concentration were selected to re-calibrate the model using the SUFI-2 method, and the number  
 460 of simulations was set to 2000. To reduce the influence of the initial value of the model parameters on the simulation results, during the model parameter calibration process, 1961 and 1962 were set as the warming-up period. Table 4 shows the evaluation metrics of the simulation using the SWAT model at a monthly scale with the largest NS value. For the calibration period from 1963 to 1990, the NSE and RE were found to be equal to 0.94 and -10.62%, respectively; for the validation period from 1991 to 2004, the model performance was slightly better than that in the calibration period, and the NSE and RE were 0.95 and -8.65%,  
 465 respectively. For the whole period from 1963 to 2004, the NSE (0.94) and RE (-9.97%) were also satisfactory. Fig. 8 shows the monthly observed and simulated streamflow at Yunjinghong station from 1963 to 2004 and the histogram of the mean monthly precipitation in the LR Basin. As seen from Fig. 8 (a) and Fig. 8 (b), the SWAT model can simulate the flow processes very well and almost perfectly match the observed streamflow curve. Note that the simulated streamflow overestimated the floods in individual years (1973, 1985 and 1995 in Fig.8 (b)), which might be caused by the uncertainty of the precipitation product (Han



470 et al., 2019). In summary, the SWAT model can better simulate the streamflow process at Yunjinghong station on a monthly scale;  
 therefore, this model is considered suitable for the next part of the research.

**Table 4** Evaluation metrics, Nash-Sutcliffe Efficiency and Relative Error of the SWAT model on a monthly scale

Period	NSE	RE (%)
Calibration (1963-1990)	0.94	-10.62
Validation (1991-2004)	0.95	-8.65
Overall (1963-2004)	0.94	-9.97



475 **Fig. 8.** Normalized monthly observed and simulated streamflow at Yunjinghong station for the calibration (from 1963 to 1990) and  
 validation (from 1991 to 2004) periods. The blue histogram shows the monthly precipitation in the LR Basin. The normalized  
 streamflow was calculated from the observed and simulated streamflow divided by their average values.

480 According to the method described in Section 3.4.2, simulations with NSEs greater than 0.75 among the 1000 simulations were  
 selected. Fig. 9 shows the number of simulations with  $0.75 \leq NSE < 0.8$ ,  $0.8 \leq NSE < 0.85$ ,  $0.85 \leq NSE < 0.9$  and  $0.9 \leq NSE <$   
 0.95 during the calibration period (1963 - 1990), the validation period (1991 - 2004) and the whole period (1963 - 2004) on a  
 monthly scale. In summary, there were 575 simulations with NSEs greater than 0.75 out of 1000 simulation results during the  
 485 calibration period, the validation period, and the whole period. Clearly, the NSEs of most simulation results were between 0.75  
 and 0.9, with 533, 537 and 533 simulations in the calibration period, the validation period, and the whole period, respectively,  
 and only a few simulation results had NSEs greater than 0.9. In the different periods, the model performed well in the validation period  
 compared with that in the calibration period, which indicated that the model has good predictive ability in the LR Basin.

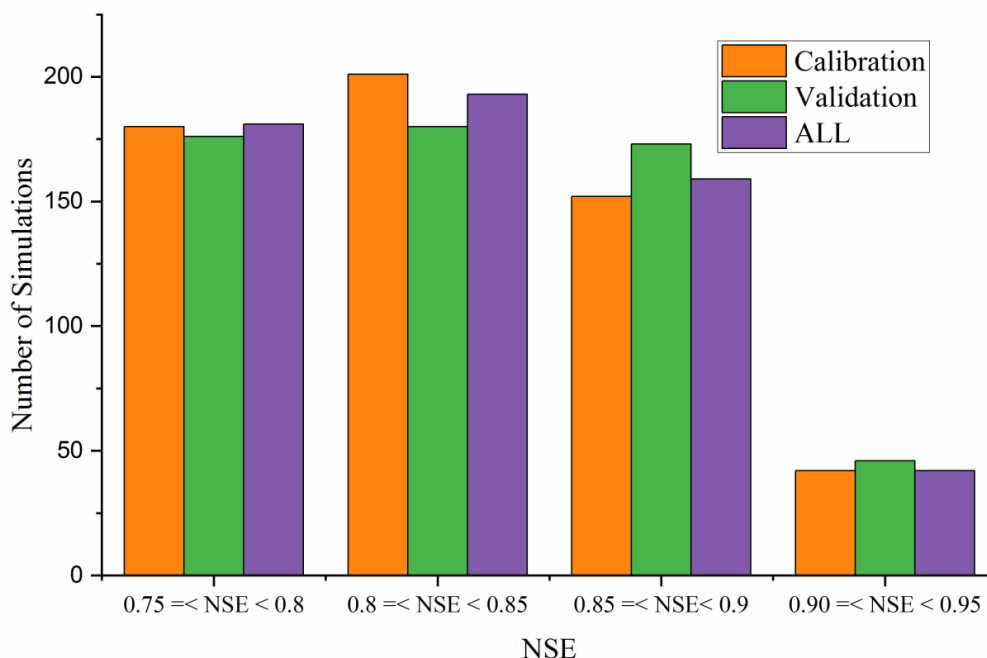


**Fig. 9.** Number of simulations with NSEs greater than 0.75 during the calibration (1963 - 1990), validation (1991 - 2004), and whole periods (1963 - 2004).

#### 4.3 Quantification of climate change and human activities for streamflow change considering the uncertainties

##### 495 4.3.1 Quantification of the impacts considering the uncertainties at the annual scale

The 575 simulations with NSEs greater than 0.75 were selected to construct the posterior histogram frequency distribution (PHD) of the contribution rate of climate change and human activities to streamflow changes in the LR Basin. Fig. 10 shows the number of simulations of the climate change contribution rate in 5% intervals and their corresponding NS box plots. In total, 167 out of 575 simulations calculated that the contribution rate of climate change in the LR Basin to runoff reduction was 40% - 45%, and the average NSE was 0.84. Then, 131 and 92 of the simulation results had calculated climate contribution rates of 35 - 40% and 45 - 50%, respectively. The contribution rate of climate change in other intervals had relatively few simulations. The NSE value of the climate change contribution rate between 70-75% was the largest (NSE = 0.86), but it had only 1 simulation. Therefore, when using hydrological simulations to quantify the contribution rate of climate change and human activities to the streamflow change of the watershed, not only the merits of the model performance but also the uncertainty of the model simulation should be considered. In general, according to the results calculated by the new quantitative framework proposed in this paper, streamflow changes in the LR Basin duo to climate change accounted for 40-45% (with an average contribution rate of 42.6%), and the corresponding human activities accounted for 55-60% (with an average contribution rate of 57.4%).

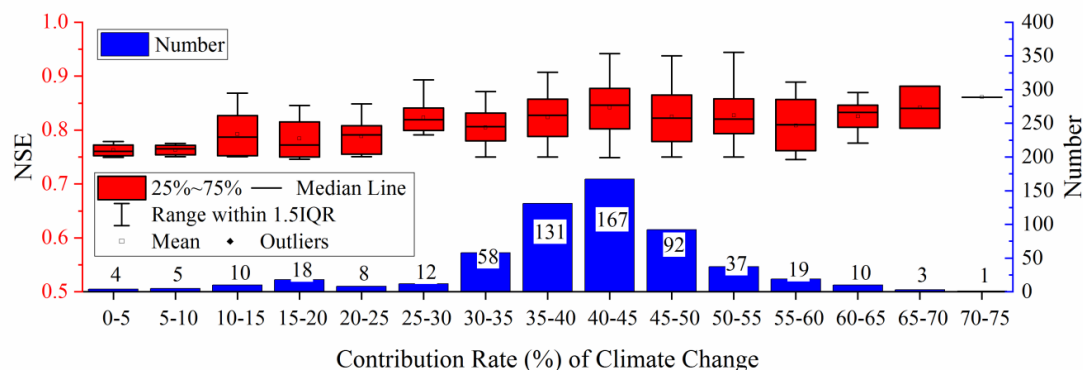


**Fig. 10.** Histogram of the number of simulations of the contribution rate (with 5% steps) of climate change to streamflow

505 reduction in the Lancang River Basin at the annual scale and corresponding Nash-Sutcliffe Efficiency box plots.

Table 5 shows the average values of the main hydrological and meteorological elements and their changes during the natural period and the impacted period. During the impacted period, compared with the natural period, the multiyear average streamflow decreased by 396 m<sup>3</sup>/s (86.5 mm), the precipitation decreased by 25 mm; as basin wide temperatures increased, the mean potential evapotranspiration and temperature in the basin increased by 6.4 mm and 0.9°C. In terms of relative changes, the streamflow decreased by 22%, but precipitation and potential evapotranspiration changed by -2.9% and 6.4%, respectively, which may indicate that the streamflow reduction in the LR Basin was mainly caused by human activities.

**Table 5** Hydrological and meteorological elements in the natural (1963 - 2004) and impacted periods (2005 - 2015) of the LR Basin and their changes during the two periods

Hydrometeorological element	Streamflow (m <sup>3</sup> /s)	Streamflow (mm)	Precipitation (mm)	PET (mm)	T (°C)
Natural period	1801.5	398.6	863.8	832.5	5.8
Impacted period	1405.5	312.1	838.8	885.8	6.7
Amount of change	-396	-86.5	-25	53.3	0.9
Relative change (%)	-22.0	-22.0	-2.9	6.4	15.9

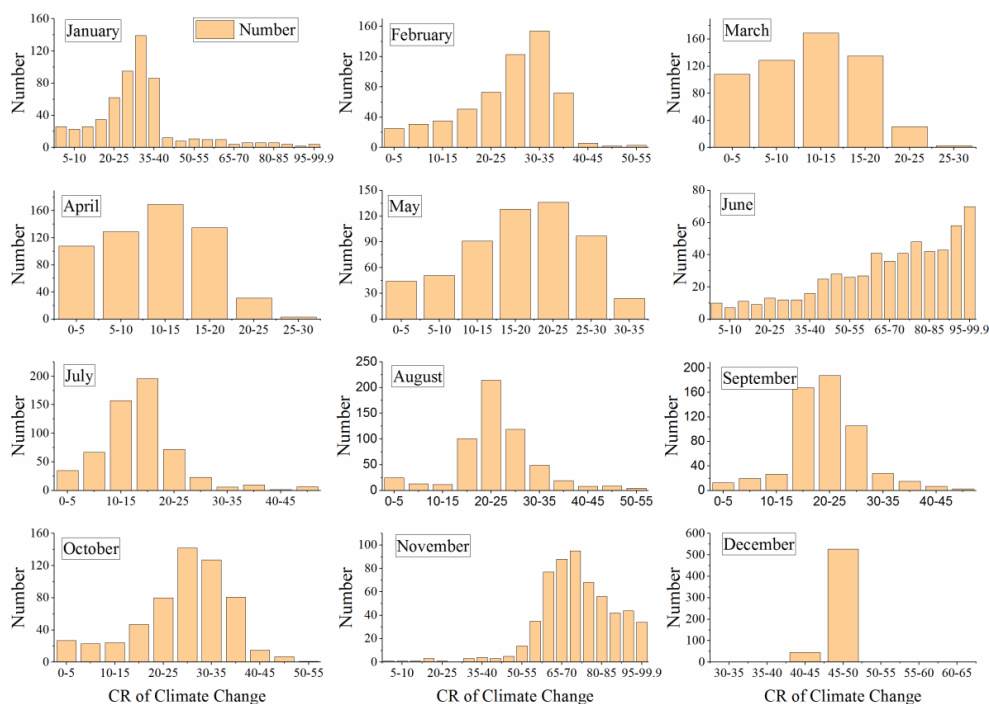
(Notation: PET = “Potential evapotranspiration” and T = “Temperature”)

#### 515 4.3.2 Quantification of the impacts considering the uncertainties on a monthly scale

The monthly contribution rate of climate change and human activities to the changing streamflow at Yunjinghong station was also analyzed using the new framework proposed in this study, and the results are shown in Fig. 11. In general, only June and November had a large contribution rate of climate change, which reached 95 - 99.9% and 70 - 75%, respectively, while the contribution rate of climate change in the other 10 months was relatively small. The trends of the streamflow and the precipitation and mean temperature in the study area shown in Fig. 5 and Fig. 7 indicate that the streamflow in June and November showed a decreasing trend (Fig. 5), while the precipitation in June decreased significantly (passing the significance level of 0.05), and the temperature increased significantly (passing the significance level of 0.05) (Fig. 7). This significant decrease in precipitation and



the significant increase in temperature were the main reasons for the decrease in the streamflow in June; that is, the decrease in the streamflow in June was mainly caused by climate change. The main factors that led to the decrease in the streamflow in November were also the decrease in precipitation and the significant increase in temperature (Fig. 7). From the results of each month, the contribution rate of climate change in March and April was the smallest, reaching 10 - 15%; followed by July (15 - 20%); May, August, and September (20 - 25%); October (25 - 30%); January and February (30 - 35%); and December (45 - 50%).



530 **Fig. 11.** Histogram of the number of simulations of the contribution rate (CR) (with 5% step) of climate change to streamflow reduction in the Lancang River Basin on a monthly scale.

The mean contribution rate of climate change and human activities at the monthly scale, which was calculated by averaging the contribution rates of all simulation results within the highest frequency, is displayed in Fig. 12 (left panel), and the monthly precipitation, potential evapotranspiration and runoff depth during the natural period and the impacted period are shown in the right panel of Fig. 12. Overall, the monthly contribution rate was consistent with the annual results, and the contribution rate in a total of 10 months was mainly due to human activities that led to a decrease in the streamflow in the LR Basin. It is worth noting that the contribution rate of climate change in June reached 96%. The panel in the right of Fig. 12 shows that the precipitation in June during the impacted period was significantly reduced compared with the natural period (with a 20.2 mm decrease). At the same time, the increase in potential evapotranspiration in June was also relatively obvious (with a 9.2 mm increase). Fig. 12 (right panel) clearly shows that the streamflow in the LR Basin during the impacted period was significantly reduced compared with the



natural period in June to October, and the precipitation had little change, except in June. Therefore, we can conclude that the main reason for the decrease in the streamflow in the LR Basin was human activities, as shown in the left panel. In this study area, the main cause of the streamflow changes was mainly due to the construction of reservoirs (such as Manwan and Xiaowan), and at the same time, the water storage of these water conservancy facilities during the flood period also provides engineering support for protecting the safety of downstream life and property. Conversely, during the dry season (from January to May), the streamflow in the impacted period showed an increasing trend compared with the natural period, and the increase in runoff during these five months was mainly due to human activities (Fig. 12, left panel), which might have been caused by the release of water from the reservoirs during the dry season. For example, in 2016, due to the influence of El Niño, the countries along the lower Mekong River all suffered severe drought. The Chinese government immediately asked the Jinghong Reservoir to release water urgently, which effectively helped downstream countries mitigate a series of possible effects caused by drought and water shortages (Li et al., 2017b).

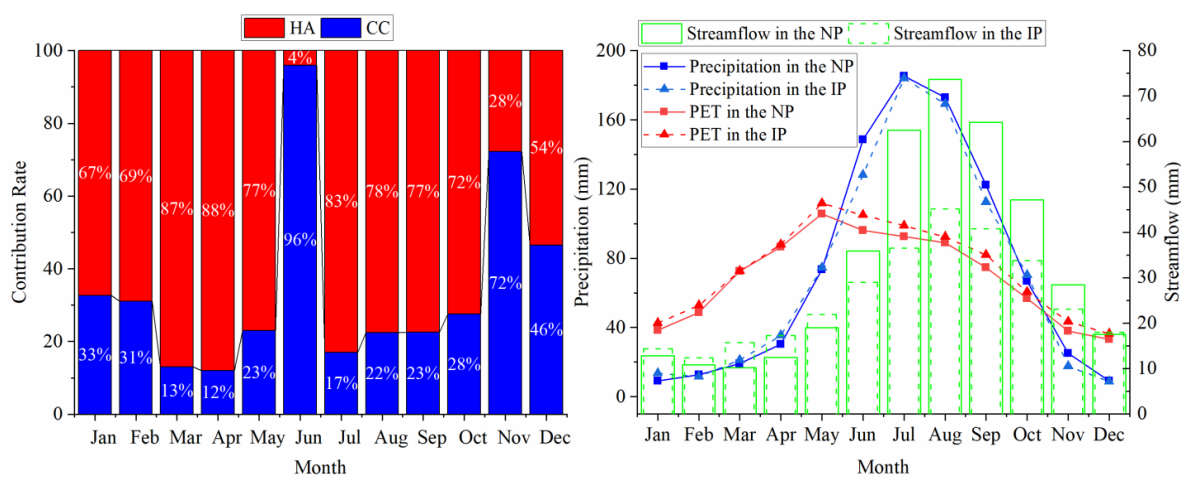


**Fig. 12.** Contribution rate of climate change and human activities to the changing monthly streamflow at Yunjinghong station (left panel), monthly precipitation, potential evapotranspiration and runoff depth during the natural period and the impacted period in the LR Basin (right panel). (Notation: HA = “Human Activities”, CC = “Climate Change”, PET = “Potential evapotranspiration”, NP = Natural Period and IP = Impacted Period)

#### 4.4 Comparison with the other two methods

In this sub-section, the new proposed framework that considers the uncertainty of hydrological simulations was compared with the Budyko framework, five sections of water withdrawal data from the LR Basin and the equivalent streamflow depth converted from the dead storage capacity of six large hydropower stations.

Table 6 shows the contribution rate of climate change and human activities to annual streamflow changes at Yunjinghong station, which was calculated from the Budyko framework. The actual evapotranspiration was calculated from the annual precipitation minus the annual streamflow depth. As shown in Table 6, compared with the natural period, the precipitation and streamflow depth in the impacted period showed a decreasing trend.



565 **Table 6** Contribution rate of climate change (CC) and human activities (HA) calculated by the Budyko framework

Time period	Precipitation (mm)	Streamflow (mm)	Actual evapotranspiration (mm)	CC (%)	HA (%)
Natural period	863.8	398.6	463.7	37.2	62.8
Impacted period	838.8	312.1	526.6		

The precipitation decreased by 25 mm and the streamflow depth decreased by 86.5 mm. In contrast, the actual evapotranspiration showed an increasing trend, which may be related to the continuous increase in temperature in recent decades. The contribution rate of climate change and human activities to streamflow changes accounted for 37.2% and 62.8%, respectively, which was basically consistent with the results calculated by the new framework proposed in this study (the difference was 5.4%).

570 Fig. 13 shows the annual water withdrawals (i.e., domestic, irrigation, livestock, manufacturing and mining) in the LR Basin during the period from 1970 to 2010 and changes in the installed capacity and dead reservoir storage from 1992 to 2015. In addition to the amount of water use for irrigation, the other four types of water use withdrawals all showed an increasing trend from 1970 to 2010, with domestic water consumption increasing the most (linear slope = 0.043). The comparison between the impacted period and the natural period showed that the other four types of water consumption, except for domestic water use, all had a larger increase in the natural period than during the impacted period. To meet the power generation needs of Southwest China and the flood control and drought resistance requirements of downstream countries, the total dead storage capacity and total installed capacity of the reservoirs from 1992 to 2015 all showed a significant increase, especially after the construction of Nuozhadu hydropower station in 2012, shown in Fig. 1.

575

580

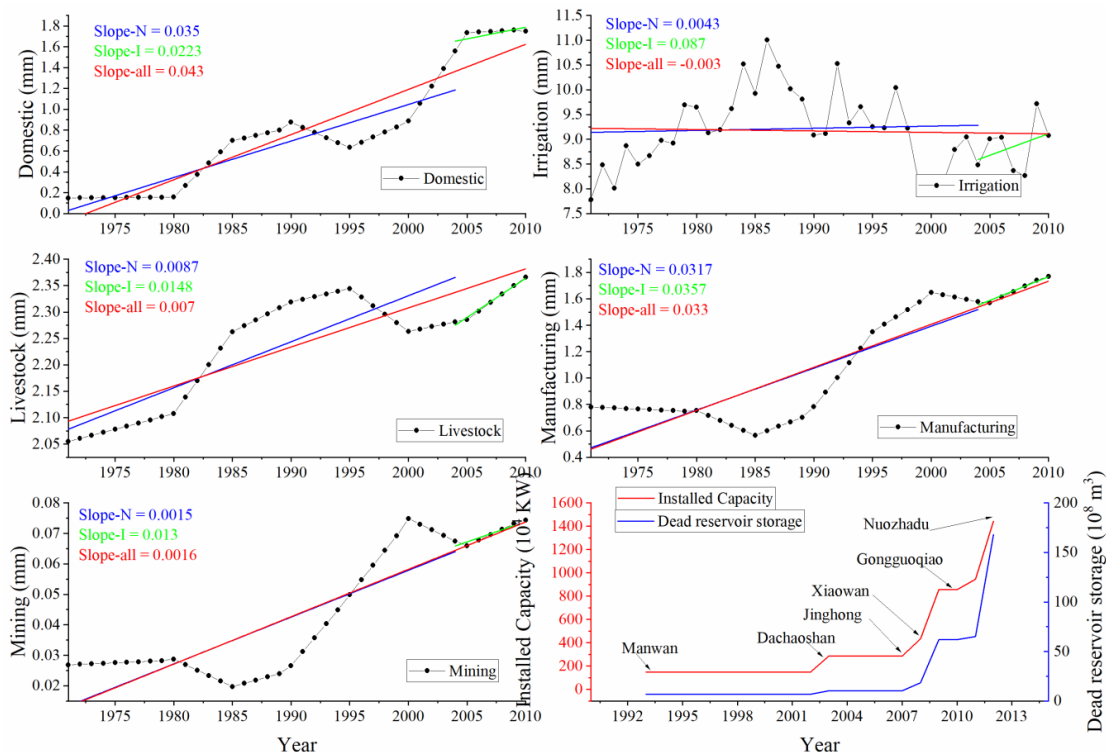


**Fig. 13.** Annual water withdrawals of the Lancang River (LR) Basin during the period from 1970 to 2010. The linear trend lines are indicated by blue (1970-2004), green (2005-2010) and red (1970-2010), and in the last panel, the total dead storage capacity and installed capacity of the LR from 1992 to 2012 are shown.

585

According to the method introduced in Section 3.5, the changes in the streamflow caused by human activities in the LR Basin were separated, which mainly included the five sections of water consumption changes and the same amount of water depth as the total dead storage capacity of the reservoir. Fig. 14 shows the contribution rate of the five types of water withdrawals by human activities and the construction of the reservoirs to the streamflow changes in the LR Basin during the impacted period (from 2005 to 2015) compared to the natural period (from 1961 to 2004). Overall, the contribution rate of human activities to streamflow changes was 59.91%, while that of climate change was 40.09%. This result was also consistent with the results calculated in Section 4.3.1. Among them, the streamflow depth caused by the construction of the reservoir was reduced by -50.17 mm, which was also the factor that had the greatest impact on streamflow compared with other human activities, and its contribution rate reached 58.0%, while the contribution rate of the other five types of water withdrawal was relatively small. The contribution rates of domestic, irrigation, livestock, manufacturing, and mining water withdrawals were 1.32%, -0.35%, 0.12%, 0.79% and 0.03%, respectively, a total of 1.91%. In other words, the decrease in the streamflow in the LR Basin was mainly due to the impact of human activities, and most of it was caused by the construction of the reservoirs.

590

595

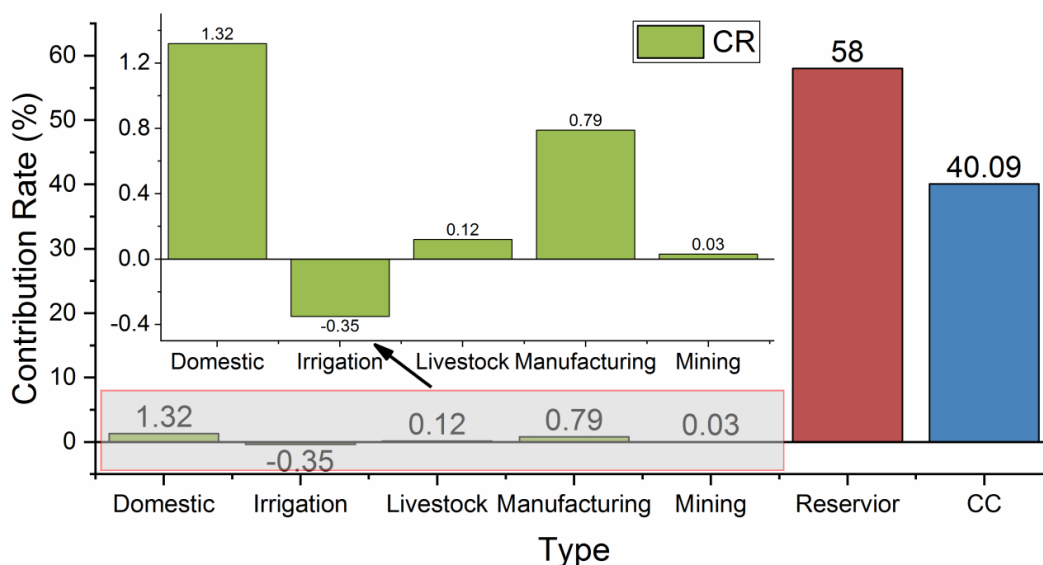


**Fig. 14.** Contribution rate (CR) of Domestic, Irrigation, Livestock, Manufacturing, and Mining water withdrawals and reservoir construction and climate change (CC) to the streamflow changes at Yunjinghong station from 1970 to 2010.

600

## 5. Discussion

### 5.1 How does parameter uncertainty affect the quantitative results?

In this paper, we proposed a novel framework to quantify the contribution rate of climate change and human activities to streamflow changes considering the uncertainty of hydrological simulations. This is because the phenomenon of "equifinality for different parameters" in hydrological simulations greatly affects the quantification results. To preliminarily investigate the impact of model simulation uncertainty of the quantitative results, we selected the two simulation results with the largest NSEs in this study for analysis. The evaluation metrics and contribution rate of climate change and human activities are shown in Table 7, which shows that both simulations can simulate the monthly streamflow at Yunjinghong station in the LR Basin accurately, and the two simulations have almost the same evaluation performance. However, the attribution analysis obtained from the two hydrological simulations showed completely different results. In the first simulation result, according to the method introduced in Section 3.4.1, the streamflow changes in the LR Basin were mainly caused by climate change, but in the second hydrological simulation, the opposite conclusion was drawn, that is, human activities dominated. These were almost the same hydrological simulation results but with opposite conclusions from the attribution analysis; this was one of the reasons why we must consider the uncertainty of the model parameters in the attribution analysis of climate change and human activities using hydrological simulations. The results of Section 4.3.1 and related published studies (Han et al., 2019) in the LR Basin show that the streamflow changes in the LR Basin were mainly caused by human activities.

610

615



**Table 7** Results of the contribution rate of climate change and human activities to runoff changes with almost equal model performance (monthly) using the SWAT model

Simulation result	Calibration		Validation		Overall		Contribution Rate (%)	
	NSE	RE (%)	NSE	RE (%)	NSE	RE (%)	CC	HA
1st simulation	0.94	-10.6	0.95	-8.6	0.94	-9.97	54.5	45.5
2nd simulation	0.94	-7.7	0.95	-8.7	0.94	-8.1	42.1	57.9

620 (Notation: CC and HA represent the climate change and human activities, respectively; NSE and RE represent the Nash-Sutcliffe efficiency coefficient and the relative error, respectively)

625 Table 8 shows the values of 9 highly sensitive parameters of the two simulation results and the streamflow values simulated by the two simulations in the natural period and the impacted period. Table 8 and the calculation methods introduced in Section 3.4.1 show that the watershed streamflow reduction caused by climate change calculated by the 1st and 2nd simulation results was -217.1 m<sup>3</sup>/s and -170.6 m<sup>3</sup>/s, respectively, which was the reason why they had opposing calculated attribution results. From the perspective of specific parameter values, the most sensitive parameter is ALPHA\_BNK, which was the base flow alpha factor for bank storage (days) characterized by the bank storage recession curve. The difference between the two calibration results was not large, and this parameter mainly controlled the baseflow process, having little effect on the average annual streamflow while the difference in CH\_K2 in the two calibration results was larger, at 303.87 and 106.12. This parameter represented the effective hydraulic conductivity of the main channel alluvial layer, which meant that the larger the CH\_K2 value is, the more likely the water in the main channel is lost to groundwater; accordingly, the streamflow production at the outlet of the watershed would decrease (Arnold et al., 2012b; Xu et al., 2016; Zhao et al., 2018b). This might also be one of the reasons that the first simulated streamflow (1617 m<sup>3</sup>/s) was slightly smaller than the second one (1667.9 m<sup>3</sup>/s). The SFTMP parameter, which was the temperature when precipitation was converted into snowfall, returned values for the first simulation and the second simulation as 2.69°C and -0.11°C, respectively; this meant that in the first simulation, more liquid precipitation was converted into a solid state and less streamflow was formed, which also led to a smaller simulated streamflow in the first simulation. The SMTMP parameter, which was the snow melt base temperature, was -4.13°C in the first simulation result and 3.73°C in the second simulation result. From basic physical knowledge, the SMTMP parameter in the second calibration result was more reasonable. Compared with other research results with similar terrain features in this study area, Debele et al. (2010) constructed the SWAT model in the high altitude area of the source of the Yellow River, China, and the SMTMP value obtained was 4°C. The difference between the two simulations was not large for the set of the other parameters (SOL\_BD, GW\_REVAP, CN2 and SOL\_K), or the parameter that controlled the baseflow (ALPHA\_BF) had little effect on the average streamflow of the basin. Based on the above, the second simulation results were consistent with the calculation results of the new framework proposed in this study. Therefore, when we choose a hydrological simulation to analyze the attribution of climate change and human activities to streamflow variations, we should clearly also consider the actual physical meaning and the uncertainties of the model parameters.



**Table 8** Values of 9 sensitivity parameters with similar simulation results and their simulated streamflow in the natural and impacted periods

Simulation No.	1st simulation	2nd simulation
V__ALPHA_BNK	0.84	0.68
V__CH_K2	303.87	106.12
V__SOL_BD	1.51	1.93
V__GW_REVAP	0.03	0.003
V__SFTMP	2.69	-0.11
R__CN2	-0.06	-0.12
R__SOL_K	0.32	0.31
V__SMTMP	-4.13	3.73
V__ALPHA_BF	0.11	0.77
Simulated streamflow in the NP (m <sup>3</sup> /s)	1617.6	1667.9
Simulated streamflow in the IP (m <sup>3</sup> /s)	1400.5	1497.3

(Notation: NP = “Natural period”, IP = “Impacted period”, R\_, V\_, and A\_ represent multiplying, replacing, and adding the corresponding parameter values, respectively, in the process of calibrating the parameters.)

## 655 5.2 Land use/land cover change in the LR Basin from 1980 to 2015

In Section 4.4, the water withdrawals of domestic, irrigation, mining, livestock, and manufacturing, and in addition, dead storage capacity of constructed reservoirs as well as the impact of human activities were separated; then the impacts of human activities on streamflow changes were separated. However, human activities also influenced the land use change on rainfall-runoff characteristics. Fig. 15 shows the land use in the LR Basin in 1980, 2000, 2010 and 2015. Farmland was the largest land use in the upper LR Basin, while the lower reaches were dominated by forest. Due to the high-altitude terrain in the upper reaches, unused land and glaciers were mainly distributed in this area. Table 9 shows the areas of land use types in the LR Basin in 1980, 1990, 2000, 2010 and 2015. In general, the water area of the LR Basin showed a significant reduction from 1980 to 1990, which was possibly due to the decrease in the area of glaciers due to the increase in temperature from 1980 to 1990 (Fig. 6). In contrast, the water area increased by nearly 30% from 2010 to 2015, which was mainly due to the construction of Nuozhadu hydropower station (with a total storage capacity of 22.7 km<sup>3</sup>) within the basin.

**Table 9** Areas (km<sup>2</sup>) of land use types in the Lancang River Basin in 1980, 1990, 2000, 2010 and 2015

Land use type	1980	1990	2000	2010	2015
Farmland	6978	6978	7034	6954	6888
Forest	33381	33633	33342	33417	33304
Grassland	42547	42652	42511	42500	42430
Water	944	593	615	615	825
City	87	112	113	129	164
Unused land	5515	5865	5837	5837	5841
Permanent glacier	724.6	206.7	247.5	247.5	243.1

The area of farmland in the LR Basin showed a decreasing trend during 2000-2010 and 2010-2015, which is also the main reason for the reduction in the irrigation water consumption in the basin, which is consistent with the results shown in Fig. 13. The areas of the cities all showed an increasing trend in the three periods of 1980-2000, 2000-2010 and 2010-2015 (by 29.8%,



670 14.1% and 27.1%, respectively), while the other three types of land use/land cover (i.e., forest, grassland, and unused land) did  
not change significantly in the three periods. In summary, no significant changes were found from 1980 to 2015 in the forest and  
grassland of the LR Basin (accounting for 37.3% and 47.5% of the total area, respectively). Although the city area has undergone  
significant changes, it accounts for a very small total area of the basin very (0.09%). The change in the water area was mainly due  
to the construction of the reservoirs, so the method used in Section 4.3 to separate the contribution of human activities to the  
675 reduction in the streamflow in the LR Basin used is reasonable.

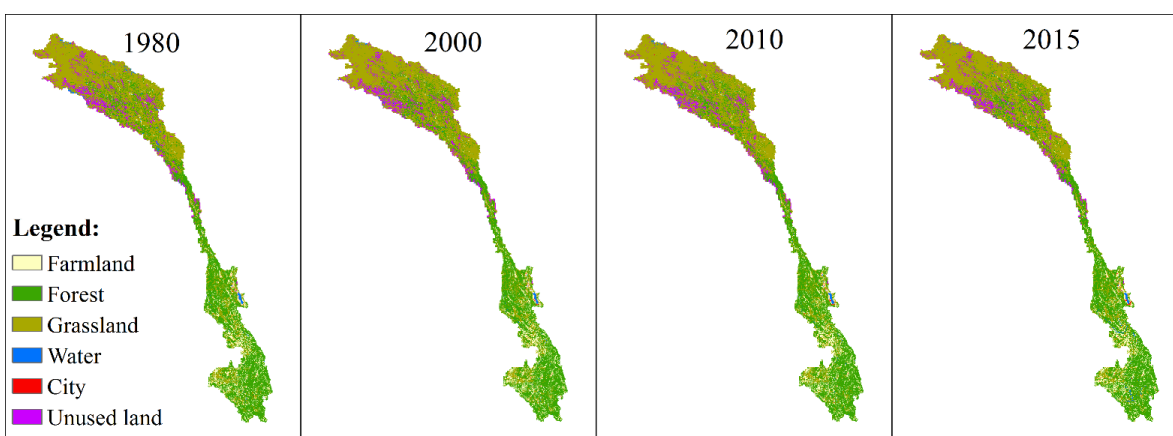


**Fig. 15.** Land use classification in the Lancang River Basin in 1980, 2000, 2010 and 2015.

### 5.3 Comparison with results of other published studies

As analyzed above, there was no particularly significant change in the precipitation and potential evapotranspiration from  
680 1961 to 2015 in the LR Basin. Human activities mainly included the construction of reservoirs, resulting in changes in the  
streamflow. Attribution analysis results showed that the contribution rate of human activities was 57.6%, and the corresponding  
climate change was 42.4%. This result was basically consistent with Han et al. (2019), but the contribution rate of human activities  
was smaller than the results of Han et al. research results (95%). This may be due to the following reasons:

1) The streamflow data of different time spans were used to obtain different break points. They used streamflow data from  
685 1980 to 2014 to obtain the break point in 2008, and this study used data from 1961 to 2015 to identify the break point in 2005.

2) Different hydrological models were used. They used the coupled routing and excess storage (CREST) model with an NSE  
of 0.57, while the SWAT model used in this study had an NSE of 0.94.

3) Longer series of streamflow data and simulation data were used.

As indicated by Li et al. (2017a) and (Han et al., 2019), as the streamflow data series became longer in the impacted period,  
690 the impact of reservoir scheduling on the streamflow changes on an average scale for many years gradually decreased. Li et al.  
(2017a) selected Chiang Saen station, which was the nearest station to Yunjinghong station downstream of the LR Basin, for their  
research, and then they divided the streamflow series into three stages, the pre-impact period (1960-1991), the transition period  
(1992-2009) and the post-impact period (2010-2014). They concluded that the construction of the reservoirs in the LR Basin led  
to a decrease in the streamflow process during the flood period and an increase in the dry period, which was consistent with the  
695 results of our study (Section 4.3.2). Their results also showed that human activities contributed 61.88% to the streamflow reduction  
at Chiang Saen station, which was also close to the results of our study (57.4%).



#### 5.4 Applicability and uncertainty of the proposed framework

A new quantitative framework for calculating the contribution rate of climate change and human activities to watershed streamflow variations was proposed in this study, and it was successfully applied to the Lancang River Basin with relatively accurate results. From our perspective, this method can effectively avoid the phenomenon of "equifinality for different parameters" that may exist in the use of hydrological simulation methods to quantify the CR of CC and HAs. At the same time, we also believe that this framework can be applied to other watersheds based on the following aspects. First, in this study, we used the Budyko framework and the sectional water withdrawal data within the basin to compare with the new framework. Second, the results of the comparison with published research on the Lancang River also proved that the framework has good accuracy and applicability. Third, in the process of comparing with the new framework, we fully considered the impact of various human activities within the study area, including five types of water withdrawals (i.e., irrigation, livestock, living, mining, and manufacturing), the impact of reservoir storage and the land use/land cover change. Of course, due to the highly nonlinear relationship between the parameters of the hydrological model, we suggest that readers ensure that the selected simulation results with NSEs greater than 0.75 are large enough when applying the novel framework in other research areas (this study had 500 simulations). Although this quantitative framework has been proved to have good applicability in the Lancang River Basin, it may also have certain limitations. First, since there is only one break point in the mean annual streamflow sequence of the Yunjinghong station in the LR basin, there may be multiple break points in other study areas. If there exists more than one break points, the results of the break point inspection of the mean annual precipitation and potential evapotranspiration in the study area, as well as the construction time of large reservoirs in the study area, should be considered (Dey and Mishra, 2017). Finally, a unique break point is selected to divide the research time series into a natural period and an impacted period, and then the quantitative framework proposed in this study can be applied. Second, because the SWAT model has good applicability at the Yunjinghong station in the LR Basin, it can meet the 500 best simulation requirements set by the framework proposed in this study, but the hydrological model may have different applicability in different research areas. Therefore, the application of this framework in other research areas may have limitations, which need to be further verified. Third, because this study uses the parameter combinations obtained by the natural period to input the meteorological element data of the impacted period for calculation, this may also bring uncertainty to the calculation results, which is usually called "transferability" (Fu et al., 2018).

Although the new quantitative framework proposed in this study considers the uncertainties in hydrological simulations, the framework is still based on traditional hydrological simulation methods to separate the contribution rate of climate change to streamflow change, and then to deduce the contribution rate of human activities. Therefore, inevitably, there are still uncertainties in the calculation process. For example, the construction of large-scale reservoirs and changes in land use/land cover (urbanization, etc.) are important factors that alter the climatic state of a local region, specifically in that they change the temporal and spatial distribution characteristics of local regional hydrometeorological elements (Degu et al., 2011; Li et al., 2017c). This change in meteorological elements was regarded as part of the impact of climate change in this study; however, it was also caused by human activities (reservoir construction). On the other hand, there are uncertainties in the division of the natural period and the impacted period in this study, which assumed that the impact of human activities on streamflow changes in the natural period was negligible; however, there were almost no periods within a watershed that were completely unaffected by human activities, and the impact of human activities on streamflow variations in the natural period was ignored in these studies. In addition, our study selected the NSE and RE as the objective function to calibrate the SWAT model, which may also bring uncertainties in the quantitative results. As indicated by Gupta et al. (2009) and Gupta and Kling (2011), using the NSE as an objective function to calibrate a hydrological



735 model may tend to underestimate the peak streamflow. Although the contribution rate in our study was calculated by the average  
streamflow over multiple years, it still brought a given amount of uncertainty to the quantitative results. Therefore, follow-up  
research should strengthen the optimization of the objective function and benefit from field investigation of the actual meaning of  
the parameters. Since the impacts of climate change and human activities on the hydrological processes of the watershed are  
740 on streamflow variations (Xin et al., 2019). Further consideration should be given to quantify the impact of specific human  
activities, such as land use change and water withdrawal, and then to separate the impact of climate change and human activities  
on streamflow changes as completely as possible.

## 6. Conclusions

In this study, we proposed a new framework that considered the uncertainties of model simulations to quantify the  
745 contribution rate of climate change and human activities to streamflow changes. This framework was developed based on the  
posterior histogram frequency distribution (PHD) of the contribution rate of climate change and human activities. Then, we  
selected the Lancang River (LR) Basin for the case study. Over the past three decades, after the construction of the Manwan  
Reservoir in 1987, six large reservoirs were constructed within the basin before 2014. The streamflow process in the watershed  
also has significant changes on multiyear average and monthly scales. The Mann-Kendall monotonic trend test and the Mann-  
750 Kendall break point test were used to test the trend and identify the break point of the annual streamflow data at Yunjinghong  
station within the period of 1961 to 2015. Then, the available period was divided into the natural period (before the break point)  
and the impacted period (after the break point). Afterwards, the SWAT model and the SUFI-2 method were used to construct the  
Posterior Histogram Distribution (PHD) of the contribution rate of climate change and human activities. Finally, the Budyko  
framework and the basin wide gridded monthly sectoral water use (GMSWU) data set were used to compare with the newly  
755 proposed framework. The main conclusions of this study are as follows:

- 1) The new proposed framework can be used to quantify the contribution rate of climate change and human activities in the LR  
Basin which can fully solve the local optimal solution for hydrological simulation parameters in current related studies. The results  
of comparison using the Budyko framework and Gridded Monthly Sectoral Water Use (GMSWU) data set also showed that the  
new framework has high accuracy (the error range is within 6%).
- 760 2) The break point of the streamflow sequence during 1961-2015 at Yunjinghong station was identified in 2005. The streamflow  
significantly decreased (~ -22%) after 2005 compared with that of the natural period (1961 - 2004), which was mainly due to the  
construction of the Xiaowan Reservoir in October 2004. Significantly reduced streamflow in the flood period and significantly  
increased streamflow during the dry period also occurred, which was mainly due to the capacity adjustment of the constructed  
reservoirs. The trend test results also showed that from 1961 to 2015, the annual streamflow in the LR Basin showed a significant  
765 decreasing trend at the  $\alpha = 0.01$  significance level, precipitation showed a nonsignificant decreasing trend, and mean temperature  
showed a significant increasing trend at the  $\alpha = 0.01$  significance level.
- 3) The quantification results calculated using the new proposed framework showed that, on an annual scale, compared with the  
natural period of 1961 – 2004, the Contribution Rate of Climate Change and Human Activities (CR of CC and HAs) were 40 -  
45% (with an average contribution rate of 42.6%) and 55 – 60% (with an average contribution rate of 57.4%), respectively. The  
770 CR of climate change and human activities derived from the Budyko framework were 37.2% and 62.8%, respectively, and the



error between the two calculation results was 5.4%. The CR of human activities calculated using the GMSWU data and the reservoirs dead capacities was 58.0%, which also proved that the new proposed framework in this study can be used in the LR Basin.

775 4) Quantitative analysis results on a monthly scale in the LR Basin showed that, except for June and November, streamflow changes in other months were caused by human activities. Further analysis showed that the streamflow in June during the impacted period decreased by 6.9 mm compared with that in the natural period, while the precipitation and potential evapotranspiration decreased and increased by 20.2 mm and 8.83 mm, respectively; the streamflow decreased by 5.34 mm in November, while the corresponding precipitation and potential evapotranspiration changed by -7.43 mm and 5.52 mm, respectively.

780 In summary, this study provides a new calculation framework that considers the uncertainty of hydrological simulations to quantify the contribution rate of climate change and human activities to streamflow changes. The results of this case study also provide a reference for understanding the dominant factors of streamflow changes in the Lancang River Basin and improving water resource management measures for the transboundary Lancang-Mekong River Basin. Of course, this new proposed framework also needs to be applied and verified in more research areas. In addition, this framework only considers the dual impacts of climate change and human activities. However, in practical applications, water resource decision makers are more  
785 willing to understand the specific impacts of human activities such as irrigation water and land use changes. Therefore, in future research, efforts should be made to expand the framework to quantify the contribution rates of individual items of climate change and human activities.

#### **Acronyms:**

790 AE – Actual Evaporation; CC – Climate Change; CGDPA – China Gauge-based Daily Precipitation Analysis; CMA – China Meteorological Administration; CR – Contribution Rate; CREST - Coupled Routing and Excess Storage; DEM - Digital Elevation Model; GMSWU - Global gridded Monthly Sectoral Water Use data set; HA – Human Activity; HRU – Hydrologic Response Unit; HWSO V1.2 – Harmonized World Soil Database Version 1.2; LR – Lancang River; NSE – Nash-Sutcliffe Efficiency coefficient; PET - Potential Evapotranspiration; PHD - Posterior Histogram Distribution; RE – Relative Error; SRTM - Shuttle Radar Topography Mission; SUFI -2: Sequential Uncertainty Fitting Procedure version 2; SWAT – Soil & Water Assessment  
795 Tool; USDA - US Department of Agriculture Research Service.

#### **Author contributions**

Xiongpeng Tang Proposed the research framework and wrote the draft manuscript. Guobin Fu and Chao Gao Improved the language of the manuscript. Guoqing Wang and Jianyun Zhang provided the data for this study. Cuishan Liu, Yanli Liu, Zhenxin Bao, Silong Zhang and Junliang Jin Jointly processed the data, helped build the hydrological model.

#### **800 Competing interests**

The authors declare that they have no conflict of interest.



### Code and data availability

The observed streamflow data from the Information Center of the Ministry of Water Resources and the local water resources management department are available upon request from the corresponding author ([gqwang@nhri.cn](mailto:gqwang@nhri.cn)) and the first author  
805 ([xptanghhu@163.com](mailto:xptanghhu@163.com)). The observed precipitation, temperature, wind speed, relative humidity data sets can be downloaded from <https://data.cma.cn/>.

### Acknowledgements

This research was financially sponsored by two research programs in China: (1) the National Key Research and Development Program (No. 2018YFC1508104), (2) the National Natural Science Foundation of China (No. 92047301, 52079079, 51879163),  
810 and, (3) the Second Tibetan Plateau Scientific Expedition and Research Program (No. 2019QZKK0203).

### References:

- Abbaspour, K.C., Genuchten, M.T.V., Schulin, R., Schläppi, E., 1997. A sequential uncertainty domain inverse procedure for estimating subsurface flow and transport parameters. *Water Resources Research*, 33(8): 1879-1892. DOI:10.1029/97WR01230
- 815 Abbaspour, K.C., Johnson, C.A., Genuchten, M.T.V., 2004. Estimating Uncertain Flow and Transport Parameters Using a Sequential Uncertainty Fitting Procedure. *Vadose Zone Journal*, 3(4): 1340-1352. DOI:10.2113/3.4.1340
- Abbaspour, K.C., Yang, J., Maximov, I., Siber, R., Bogner, K., Mieleitner, J., Zobrist, J., Srinivasan, R., 2007. Modelling hydrology and water quality in the pre-alpine/alpine Thur watershed using SWAT. *J Hydrol*, 333(2): 413-430. DOI:10.1016/j.jhydrol.2006.09.014
- 820 Arnold, J.G., Kiniry, J.R., Srinivasan, R., Williams, J.R., Haney, E.B., Neitsch, S.L., 2012a. Soil & Water Assessment Tool: Input/Output Documentation. Version 2012. Texas Water Resources Institute, College Station, 1-650 pp.
- Arnold, J.G., Moriasi, D.N., Gassman, P.W., Abbaspour, K.C., White, M.J., Srinivasan, R., Santhi, C., Harmel, R., Van Griensven, A., Van Liew, M.W., 2012b. SWAT: Model use, calibration, and validation. *Transactions of the ASABE*, 55(4): 1491-1508. DOI:10.13031/2013.42246
- 825 Arnold, J.G., Srinivasan, R., Muttiah, R.S., Williams, J.R., 1998. Large area hydrologic modeling and assessment part I: model development. *JAWRA Journal of the American Water Resources Association*, 34(1): 73-89. DOI:10.1111/j.1752-1688.1998.tb05961.x
- Bao, Z.X., Zhang, J.Y., Wang, G.Q., Fu, G.B., He, R.M., Yan, X.L., Jin, J.L., Liu, Y.L., Zhang, A.J., 2012. Attribution for decreasing streamflow of the Haihe River basin, northern China: Climate variability or human activities? *J Hydrol*, 460: 117-129. DOI:10.1016/j.jhydrol.2012.06.054
- 830 Beven, K., 2006. A manifesto for the equifinality thesis. *J Hydrol*, 320(1-2): 18-36. DOI:10.1016/j.jhydrol.2005.07.007
- Beven, K., Binley, A., 1992. The future of distributed models: model calibration and uncertainty prediction. *Hydrological processes*, 6(3): 279-298. DOI:10.1002/hyp.3360060305
- Budyko, M.I., 1961. The heat balance of the earth's surface. *Soviet Geography*, 2(4): 3-13. DOI:10.1080/00385417.1961.10770761
- 835 Chandresis, A., Looy, K.V., Diamond, J.S., Souchon, Y., 2019. Small dams alter thermal regimes of downstream water. *Hydrol Earth Syst Sc.* 23(11): 4509-4525. DOI:10.5194/hess-23-4509-2019
- Debele, B., Srinivasan, R., Gosain, A., 2010. Comparison of process-based and temperature-index snowmelt modeling in SWAT. *Water Resour Manag*, 24(6): 1065-1088. DOI:10.1007/s11269-009-9486-2
- 840 Degu, A.M., Hossain, F., Niyogi, D., Pielke Sr, R., Shepherd, J.M., Voisin, N., Chronis, T., 2011. The influence of large dams on surrounding climate and precipitation patterns. *Geophysical Research Letters*, 38(4). DOI:10.1029/2010GL046482
- Dey, P., Mishra, A., 2017. Separating the impacts of climate change and human activities on streamflow: A review of methodologies and critical assumptions. *J Hydrol*, 548: 278-290. DOI:10.1016/j.jhydrol.2017.03.014
- 845 Farsi, N., Mahjouri, N., 2019. Evaluating the contribution of the climate change and human activities to runoff change under uncertainty. *J Hydrol*, 574: 872-891. DOI:10.1016/j.jhydrol.2019.04.028
- Fu, G., Charles, S.P., Chiew, F.H., Ekström, M., Potter, N.J., 2018. Uncertainties of statistical downscaling from predictor selection: Equifinality and transferability. *Atmospheric research*, 203: 130-140.



- Fu, G., Chen, S., Liu, C., Shepard, D., 2004. Hydro-climatic trends of the Yellow River basin for the last 50 years. *Climatic Change*, 65(1-2): 149-178. DOI:10.1023/B:CLIM.0000037491.95395.bb
- 850 Gao, C., Liu, L., Ma, D., He, K., Xu, Y.-P., 2019. Assessing responses of hydrological processes to climate change over the southeastern Tibetan Plateau based on resampling of future climate scenarios. *Science of the Total Environment*, 664: 737-752. DOI:10.1016/j.scitotenv.2019.02.013
- Gilbert, R.O., 1987. *Statistical methods for environmental pollution monitoring*. John Wiley & Sons.
- Grumbine, R.E., Xu, J., 2011. Mekong Hydropower Development. *Science*, 332(6026): 178-179. DOI:10.1126/science.1200990
- 855 Gupta, H.V., Kling, H., 2011. On typical range, sensitivity, and normalization of Mean Squared Error and Nash-Sutcliffe Efficiency type metrics. *Water Resources Research*, 47(10). DOI:10.1029/2011WR010962
- Gupta, H.V., Kling, H., Yilmaz, K.K., Martinez, G.F., 2009. Decomposition of the mean squared error and NSE performance criteria: Implications for improving hydrological modelling. *J Hydrol*, 377(1-2): 80-91. DOI:10.1016/j.jhydrol.2009.08.003
- 860 Hamed, K.H., Ramachandra Rao, A., 1998. A modified Mann-Kendall trend test for autocorrelated data. *J Hydrol*, 204(1): 182-196. DOI:10.1016/S0022-1694(97)00125-X
- Han, Z., Long, D., Fang, Y., Hou, A., Hong, Y., 2019. Impacts of climate change and human activities on the flow regime of the dammed Lancang River in Southwest China. *J Hydrol*, 570: 96-105. DOI:10.1016/j.jhydrol.2018.12.048
- Hegerl, G., Black, E., Allan, R., Ingram, W., Polson, D., Trenberth, K., Chadwick, R., Arkin, P., Sarojini, B., Becker, A., 2015. 865 Challenges in quantifying changes in the global water cycle. *Bulletin of the American Meteorological Society*, 100(10): 1097-1115. DOI:10.1175/BAMS-D-13-00212.1
- Hennig, T., Wang, W., Feng, Y., Ou, X., He, D., 2013. Review of Yunnan's hydropower development. Comparing small and large hydropower projects regarding their environmental implications and socio-economic consequences. *Renewable and Sustainable Energy Reviews*, 27: 585-595. DOI:10.1016/j.rser.2013.07.023
- 870 Huang, Z., Hejazi, M., Li, X., Tang, Q., Vernon, C., Leng, G., Liu, Y., Döll, P., Eisner, S., Gerten, D., Hanasaki, N., Wada, Y., 2018. Reconstruction of global gridded monthly sectoral water withdrawals for 1971–2010 and analysis of their spatiotemporal patterns. *Hydrol. Earth Syst. Sci.*, 22(4): 2117-2133. DOI:10.5194/hess-22-2117-2018
- Jacobs, J.W., 2002. *The Mekong River Commission: Transboundary Water Resources Planning and Regional Security*. *Geographical Journal*, 168(4): 354-364. DOI:10.1111/j.0016-7398.2002.00061.x
- 875 Kendall, M., 1975. *Rank correlation methods* (4th edn.) Charles Griffin. San Francisco, CA, 8.
- Kong, D., Miao, C., Wu, J., Duan, Q., 2016. Impact assessment of climate change and human activities on net runoff in the Yellow River Basin from 1951 to 2012. *Ecological Engineering*, 91: 566-573. DOI:10.1016/j.ecoleng.2016.02.023
- Lee, S., Yeo, I.Y., Sadeghi, A.M., Mccarty, G.W., Hively, W.D., Lang, M.W., Sharifi, A., 2018. Comparative analyses of hydrological responses of two adjacent watersheds to climate variability and change using the SWAT model. *Hydrology & Earth System Sciences*, 22: 689-708. DOI:10.5194/hess-22-689-2018
- 880 Li, D., Long, D., Zhao, J., Lu, H., Hong, Y., 2017a. Observed changes in flow regimes in the Mekong River basin. *J Hydrol*, 551: 217-232. DOI:10.1016/j.jhydrol.2017.05.061
- Li, L.J., Zhang, L., Wang, H., Wang, J., Yang, J.W., Jiang, D.J., Li, J.Y., Qin, D.Y., 2007. Assessing the impact of climate variability and human activities on streamflow from the Wuding River basin in China. *Hydrological Processes: An International Journal*, 21(25): 3485-3491. DOI:10.1002/hyp.6485
- 885 Li, Y., Li, Z., Dai, M., Wei, L., 2017b. Effect evaluation of emergency water supplement from cascade reservoirs on Lancang River to Mekong River in 2016. *Yangtze River* (in Chinese), 48(23): 56-60.
- Li, Y., Zhou, W., Chen, X., Fang, D., Zhang, Q., 2017c. Influences of the Three Gorges Dam in China on precipitation over surrounding regions. *Journal of Meteorological Research*, 31(4): 767-773. DOI:10.1007/s13351-017-6177-4
- 890 Liu, J., Zhang, Q., Singh, V.P., Shi, P., 2017. Contribution of multiple climatic variables and human activities to streamflow changes across China. *J Hydrol*, 545: 145-162. DOI:10.1016/j.jhydrol.2016.12.016
- Liu, J., Zhou, Z., Yan, Z., Gong, J., Jia, Y., Xu, C.-Y., Wang, H., 2019. A new approach to separating the impacts of climate change and multiple human activities on water cycle processes based on a distributed hydrological model. *J Hydrol*, 578: 124096. DOI:10.1016/j.jhydrol.2019.124096
- 895 Liu, Q., Liang, L., 2015. Impacts of climate change on the water balance of a large nonhumid natural basin in China. *Theoretical and applied climatology*, 121(3-4): 489-497. DOI:10.1007/s00704-014-1255-3
- Malagò, A., Pagliero, L., Bouraoui, F., Franchini, M., 2015. Comparing calibrated parameter sets of the SWAT model for the Scandinavian and Iberian peninsulas. *Hydrological Sciences Journal*, 60(5): 949-967. DOI:10.1080/02626667.2014.978332
- 900 Mann, H.B., 1945. Nonparametric tests against trend. *Econometrica: Journal of the Econometric Society*: 245-259. DOI:10.2307/1907187
- Moriasi, D.N., Arnold, J.G., Van Liew, M.W., Bingner, R.L., Harmel, R.D., Veith, T.L., 2007. Model evaluation guidelines for systematic quantification of accuracy in watershed simulations. *Transactions of the ASABE*, 50(3): 885-900. DOI:10.13031/2013.23153



- 905 Nash, J.E., Sutcliffe, J.V., 1970. River flow forecasting through conceptual models part I—A discussion of principles. *J Hydrol*, 10(3): 282-290. DOI:10.1016/0022-1694(70)90255-6
- Piman, T., Cochrane, T., Arias, M., 2016. Effect of proposed large dams on water flows and hydropower production in the Sekong, Sesan and Srepok rivers of the Mekong Basin. *River research and applications*, 32(10): 2095-2108. DOI:10.1002/rra.3045
- 910 Piman, T., Cochrane, T., Arias, M., Green, A., Dat, N., 2012. Assessment of flow changes from hydropower development and operations in Sekong, Sesan, and Srepok rivers of the Mekong basin. *Journal of Water Resources Planning and Management*, 139(6): 723-732. DOI:10.1061/(ASCE)WR.1943-5452.0000286
- Shen, Y., Zhao, P., Pan, Y., Yu, J., 2014. A high spatiotemporal gauge-satellite merged precipitation analysis over China. *Journal of Geophysical Research: Atmospheres*, 119(6): 3063-3075. DOI:10.1002/2013JD020686
- 915 Sneyers, R., 1991. On the statistical analysis of series of observations.
- Song, X., Zhang, J., Zou, X., Zhang, C., AghaKouchak, A., Kong, F., 2019. Changes in precipitation extremes in the Beijing metropolitan area during 1960–2012. *Atmospheric Research*, 222: 134-153. DOI:10.1016/j.atmosres.2019.02.006
- Tang, G., Long, D., Hong, Y., Gao, J., Wan, W., 2018. Documentation of multifactorial relationships between precipitation and topography of the Tibetan Plateau using spaceborne precipitation radars. *Remote Sensing of Environment*, 208: 82-96. DOI:10.1016/j.rse.2018.02.007
- 920 Tang, X., Zhang, J., Wang, G., Yang, Q., Yang, Y., Guan, T., Liu, C., Jin, J., Liu, Y., Bao, Z., 2019. Evaluating Suitability of Multiple Precipitation Products for the Lancang River Basin. *Chinese Geographical Science*, 29(1): 37-57. DOI:10.1007/s11769-019-1015-5
- Teuling, A.J., De Batts, E.A., Jansen, F.A., Fuchs, R., Buitink, J., Van Dijke, A.J.H., Sterling, S.M., 2019. Climate change, reforestation/afforestation, and urbanization impacts on evapotranspiration and streamflow in Europe. *Hydrol Earth Syst Sc*, 23(9): 3631-3652. DOI:10.5194/hess-23-3631-2019
- Tilt, B., Gerkey, D., 2016. Dams and population displacement on China's Upper Mekong River: Implications for social capital and social-ecological resilience. *Global Environmental Change*, 36: 153-162. DOI:10.1016/j.gloenvcha.2015.11.008
- Tuo, Y., Duan, Z., Disse, M., Chiogna, G., 2016. Evaluation of precipitation input for SWAT modeling in Alpine catchment: A case study in the Adige river basin (Italy). *Science of the Total Environment*, 573: 66-82. DOI:10.1016/j.scitotenv.2016.08.034
- 930 Wang, G.Q., Zhang, J.Y., Pagano, T.C., Liu, Y.L., Liu, C.S., Bao, Z.X., Jin, J.L., He, R.M., 2015. Using hydrological simulation to detect human-disturbed epoch in runoff series. *Water Sci Technol*, 71(5): 691-699. DOI:10.2166/wst.2014.526
- Wang, W., Shao, Q., Yang, T., Peng, S., Xing, W., Sun, F., Luo, Y., 2013. Quantitative assessment of the impact of climate variability and human activities on runoff changes: a case study in four catchments of the Haihe River basin, China. *Hydrological Processes*, 27(8): 1158-1174. DOI:10.1002/hyp.9299
- 935 Wu, H., Chen, B., 2015. Evaluating uncertainty estimates in distributed hydrological modeling for the Wenjing River watershed in China by GLUE, SUFI-2, and ParaSol methods. *Ecological Engineering*, 76: 110-121. DOI:10.1016/j.ecoleng.2014.05.014
- 940 Xie, J., Xu, Y.-P., Wang, Y., Gu, H., Wang, F., Pan, S., 2019. Influences of climatic variability and human activities on terrestrial water storage variations across the Yellow River basin in the recent decade. *J Hydrol*, 579: 124218. DOI:10.1016/j.jhydrol.2019.124218
- Xie, P., Yatagai, A., Chen, M., Hayasaka, T., Fukushima, Y., Liu, C., Yang, S., 2007. A Gauge-Based Analysis of Daily Precipitation over East Asia. *Journal of Hydrometeorology*, 8(3): 607-626. DOI:10.1175/JHM583.1
- 945 Xin, Z., Li, Y., Zhang, L., Ding, W., Ye, L., Wu, J., Zhang, C., 2019. Quantifying the relative contribution of climate and human impacts on seasonal streamflow. *J Hydrol*, 574: 936-945. DOI:10.1016/j.jhydrol.2019.04.095
- Xu, H., Xu, C.Y., Chen, S., Chen, H., 2016. Similarity and difference of Global reanalysis datasets (WFD and APHRODITE) in driving lumped and distributed hydrological models in a humid region of China. *J Hydrol*, 542: 343-356. DOI:10.1016/j.jhydrol.2016.09.011
- 950 Xu, M., Kang, S., Wu, H., Yuan, X., 2018. Detection of spatio-temporal variability of air temperature and precipitation based on long-term meteorological station observations over Tianshan Mountains, Central Asia. *Atmospheric Research*, 203: 141-163. DOI:10.1016/j.atmosres.2017.12.007
- Xue, Z., Liu, J.P., Ge, Q., 2011. Changes in hydrology and sediment delivery of the Mekong River in the last 50 years: connection to damming, monsoon, and ENSO. *Earth Surface Processes & Landforms*, 36(3): 296-308. DOI:10.1002/esp.2036
- 955 Yang, J., Reichert, P., Abbaspour, K.C., Xia, J., Yang, H., 2008. Comparing uncertainty analysis techniques for a SWAT application to the Chaohe Basin in China. *J Hydrol*, 358(1): 1-23. DOI:10.1016/j.jhydrol.2008.05.012
- Yang, L., Feng, Q., Yin, Z., Wen, X., Si, J., Li, C., Deo, R.C., 2017. Identifying separate impacts of climate and land use/cover change on hydrological processes in upper stream of Heihe River, Northwest China. *Hydrological Processes*, 31(5): 1100-1112. DOI:10.1002/hyp.11098
- 960 Zhang, L., Dawes, W., Walker, G., 2001. Response of mean annual evapotranspiration to vegetation changes at catchment scale. *Water resources research*, 37(3): 701-708. DOI:10.1029/2000WR900325



- Zhao, F., Wu, Y., Qiu, L., Sivakumar, B., Zhang, F., Sun, Y., Sun, L., Li, Q., Voinov, A., 2018a. Spatiotemporal features of the hydro-biogeochemical cycles in a typical loess gully watershed. *Ecological Indicators*, 91: 542-554. DOI:10.1016/j.ecolind.2018.04.027
- 965 Zhao, F., Wu, Y., Qiu, L., Sun, Y., Sun, L., Li, Q., Niu, J., Wang, G., 2018b. Parameter uncertainty analysis of the SWAT model in a mountain-loess transitional watershed on the Chinese Loess Plateau. *Water-Sui*, 10(6): 690. DOI:10.3390/w10060690
- Zhao, Q., Liu, S., Deng, L., Dong, S., Yang, J., Wang, C., 2012. The effects of dam construction and precipitation variability on hydrologic alteration in the Lancang River Basin of southwest China. *Stochastic Environmental Research & Risk Assessment*, 26(7): 993-1011. DOI:10.1007/s00477-012-0583-z
- 970